Data fusion is the process of putting together information obtained from many heterogeneous sensors, on many platforms, into a single composite picture. Data fusion researches focuses on the development of models appropriate to unify images have different scale with complex information. In this book, many fusion techniques have been used to improve low resolution remotely sensed images, and renewing the information by considering that the high resolution images are newer than the restored image. The unifying methods used are: 1.Fusion techniques based on wavelet transformations; The Haar and the Tap 3/5 wavelet transformations. 2.Lab, HLS, and YUV color transformation algorithms were used for the unification purposes, and finally 3.The Principle Component Analysis (PCA) transformation technique is used to perform the fusion. The produced image quality have been tested, subjectively by showing the obtained results, and quantitatively by measuring the Normalized-Mean-Square-Error (NMSE), the Signal-to-Noise-Ratio (SNR), and the Peak-Signal-to-Noise-Ratio (PSNR) of the output images compared with the large-scale panchromatic SPOT scene.

Dr.Firas A.Hadi was born in Baghdad-Iraq. He studied at University of Baghdad where he completed two degrees: B.Sc. in Physics, M.Sc. in Image processing. He obtained his Ph.D. at Al-Nahrai University in 2015.He is a contributor to many journals and conferences. He was working Ministry of Science and Tech. and Now at AL_Karkh University of Science.

978-3-659-97996-5

An integrated methods

Firas A. Hadi
Rawnak A. Abdulwahhab

Unifying Technique for Multisource Remote Sensing Images

A. Hadi, A. Abdulwahhab

LAP LAMBERT Academic Publishing

Firas A. Hadi
Rawnak A. Abdulwahhab

Unifying Technique for Multisource Remote Sensing Images

Firas A. Hadi
Rawnak A. Abdulwahhab

Unifying Technique for Multisource Remote Sensing Images

LAP LAMBERT Academic Publishing

Impressum / Imprint
Bibliografische Information der Deutschen Nationalbibliothek: Die Deutsche Nationalbibliothek verzeichnet diese Publikation in der Deutschen Nationalbibliografie; detaillierte bibliografische Daten sind im Internet über http://dnb.d-nb.de abrufbar.

Bibliographic information published by the Deutsche Nationalbibliothek: The Deutsche Nationalbibliothek lists this publication in the Deutsche Nationalbibliografie; detailed bibliographic data are available in the Internet at http://dnb.d-nb.de.

Coverbild / Cover image: www.ingimage.com

Verlag / Publisher:
LAP LAMBERT Academic Publishing
ist ein Imprint der / is a trademark of
OmniScriptum GmbH & Co. KG
Bahnhofstraße 28, 66111 Saarbrücken, Deutschland / Germany
Email: info@omniscriptum.com

Herstellung: siehe letzte Seite /
Printed at: see last page
ISBN: 978-3-659-97996-5

Unifying Technique for Multisource Remote Sensing Images

By

Dr. Firas A. Hadi

Rawnak A. Abdulwahab

Acknowledgments

*Firstly, I would like to praise to **ALLAH (the Great and Almighty)** for his graces that enable me to continue the requirements of my study.*

I would like to submit my sincere thanks to my supervisor Dr. Saleh M. Ali for his helpful comments, valuable suggestions, advices and encouragement.

*Also much gratefulness for Dr. Alaa S. Mahdi, staff of **Remote Sensing Unit, the achievement of Physics Department and the College of Science.** I would like to thank all the benevolent hands that lend me a helping in this project.*

Finally …

I pray to Allah (the Great and Almighty)

To bless the all

Contents

List of Abbreviations

1DWT	One-Dimensional Wavelet Transform
2DWT	Two-Dimensional Wavelet Transform
CIE	Commission International de l'Éclairage
CIELab	CIE the Lab for lightness and ***a*** and ***b*** for the color-opponent dimensions
CIELuv	Commission International de l'Éclairage on Illumination
CNES	Centre National D'Etudes Spatiales.
CRT	Cathod Ray Tube.
CWT	Continuous Wavelet Transform.
dB	Decibels.
DWT	Discrete Wavelet Transform.
EMR	Electromagnetic Radiation.
EOSAT	Earth Observation Satellite.
EROS	Earth Resource Observation System.
ERTS	Earth Resource Technology Satellite.
ETM+	Enhanced Thematic Mapper Plus.
HCI	Hue-(chroma / colorfulness) – intensity.
HEO	High Earth Orbit.
HSI	Hue-Saturation-Intensity.
HISS	High Speed Sentry.
HLS	Hue-Lightness-Saturation.
HPF	High Pass Filter.
HRV	High Resolution Visible.
HSV	Hue-Saturation Value.
HVC	Hue-value- colorfulness.
HVS	Human Visual System.
IFOV	Instantaneous Field of View.
IR	Infra-Red.
IRS	Indian Remote Sensing.
JPEG	Joint Photographic Experts Group
KL	Karhunen-Loeve.
LEO	Low Earth orbit.
MEO	Medium Earth Orbit.
MS	Multispectral.
MSE	Mean Square Error.

MSS	Multispectral Scanner.
NASA	National Aeronautics and Space Administration.
NMSE	Normalized Mean Square Error.
NOAA	National Oceanic and Atmospheric Administration.
NTSC	National Television System Committee.
PAL	Phase Alternation Line.
PAN	Panchromatic.
PCA	Principal component Analysis.
PCT	Principal Components Transform.
PSNR	Peak-Signal to Noise Ratio.
RGB	Red, Green, Blue.
RMSE	Root Mean Square Error.
SAR	Synthetic Aperture Radar.
SECAM	Sequence de Couleurs Avec Memoire.
SNR	Signal-to-Noise Ratio.
SNSB	Swedish National Space Board.
SPOT	Satellite Pour I' Observation de la Terra.
SPOT XS	Satellite Pour I' Observation de la Terra with sort of XS multispectral scanner.
SSTC	Scientific, Technical, and Cultural Services.
TM	Thematic Mapper.
TSD	Hue- saturation – darkness.
USGS	United State Geological Servey.
USSR	Union of Soviet Socialist Republics.
VIR	Visible Infrared.
WT	Wavelet Transformation.
YC_bC_r	Y or luminance/intensity signal, it contains the main picture information, C_b and C_r are first chrominance blue and first chrominance red respectively.
YCC	abbreviated to YC_bC_r.
YIQ	Y is same above, Inphase Quadrature.
YUV	Y is same above, U is Hue, and V is Saturation.

Abstract

Data fusion is the process of putting together information obtained from many heterogeneous sensors, on many platforms, into a single composite picture. Data fusion researches focuses on the development of models appropriate to unify images have different scale with complex information.

In this research, many fusion techniques have been used to improve small scale (low resolution) remotely sensed images, and renewing the information by considering that the large scale (high resolution) images are newer than the restored image. The unifying methods used are:

1. Fusion techniques based on wavelet transformations; The Haar and the Tap 3/5 wavelet transformations have been adopted and used with several transformation levels. The small scale Low-Low scenes are replaced by the Low-Low of the large scale scenes for the corresponding transformation level. Inverse wavelet transformation then implemented to reconstruct the enhanced scenes.
2. Three color transformation methods were used to improve the lower scale remotely sensed scenes; The Lab, HLS, and YUV color transformation algorithms have been adopted for the unification purposes. The most energetic color band; i.e. L-band of the Lab, L-band of the HLS, and the Y-band of the YUV have been replaced by the larger scale scenes (the Panchromatic of the SPOT image). Inverse color transformation then implemented to reconstruct the enhanced scenes.
3. The Principle Component Analysis (PCA) transformation technique is used to perform the fusion (i.e. Unification) method. This transformation represents the optimum transformation, in the sense; it is yielding maximum de-correlation. The 1st PCA of the lower scale scenes is replaced by the larger scale scene (i.e. the Panchromatic of the SPOT image). Inverse PCA transformation is used to reconstruct the enhanced fused images.

   The produced image quality have been tested, subjectively by showing the obtained results, and quantitatively by measuring the Normalized-Mean-Square-Error (NMSE), the Signal-to-Noise-Ratio (SNR), and the Peak-Signal-to-Noise-Ratio (PSNR) of the output images compared with the large-scale panchromatic SPOT scene.

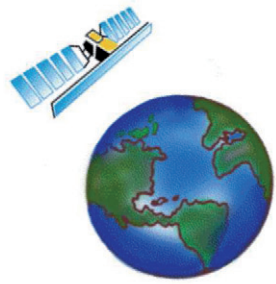

CHAPTER ONE

General introduction

GENERAL INTRODUCTION

1.1 Preface

Many types of remote sensing images are routinely recorded in digital form and then processed by computers to produce images for interpreters to study. The simplest form of digital image processing employs a micro-processor that convert the digital data into a film image with minimal corrections and calibrations. At the other extreme, some dedicated computers systems are employed for sophisticated interactive manipulation of the data to produce images in which specific in information has been produced and highlighted [Sab 1978].

Remote sensing system, particularly those deployed on satellite, provides a repetitive and consistent view of earth that is invaluable to monitoring the earth system and the effects of human activities on the earth. Some of the important applications of remote sensing technology are:-

- Environmental assessment and monitory (urban growth).
- Change detection and monitoring (atmospheric ozone).
- Agriculture (crop condition, yield production, soil erosion).
- Resource exploration (minerals, oil, nature gas).
- Natural resources (wetlands, soils, forest, oceans).
- Mapping (topography, land use, and civil engineering).
- Military surveillance and reconnaissance (strategic, policy, tactical assessment) [Azz 2001].

To utilized satellite images in different branches of applications, there was a real need to develop the mathematical structure as well as the algorithms that could be results [Azz 2001]. This requirement was started with the initial impetus program of unmanned planetary satellites in the 1960s that telemeter, transmitted, images to ground receiving stations. The low quality of the received images required the development of processing techniques to make the images useful.

Another impetus was the Landsat program, which began in 1972 provided worldwide coverage in digital format. A third impetus is the continued development of faster and more powerful computers with software that are suitable for image processing [Sab 1978].

1.2 Aim of the Project

The aim of book is to study the unifying techniques and obtain results for unifying SPOT and ETM+ with new high spatial and spectral resolution for ETM+ image.

1.3 Literature Review

In the mid-1980s, image fusion received significant attention from researchers in remote sensing and image processing fields, the French satellite carries SPOT 1 (lunched in 1986) provide multi-resolution images; i.e., moderate resolution images of 20m, and Pan high-resolution images of 10m. Since then, many researches have been developed to improve the lower resolution images by introducing fusion techniques. Among the variations of image fusion techniques, the most popular and effective are, for example, HSI (Hue, Saturation, and Intensity), PCA (Principal Components Analysis), arithmetic combinations, and wavelet base fusion.

While Chavez *et al.* (1991) [Cha 1991] :explain the HSI, PCA, HPF (High-Pass Filter) methods to merge multi-resolution and multi-spectral data (Landsat TM, SPOT Panchromatic) and comparison the methods. The authors discovered that the Hue-Saturation-Intensity "HSI" method distorting the spectral characteristics of the processed data. This degradation effects is reduced when applying the PCA fusion method, and effectively attenuated by applying the HPF method.

Garguct-Duport *et al. (*1996)[Gar 1996]: attempted to perform image merging, using multi-resolution analysis based on the wavelet transform which was applied on SPOT PAN and SPOT XS sensed images. This method is compared with the HSI method, using three criteria; i.e. ***geometrical improvement***, ***preservation of spectral characteristics***, and ***thematic analysis***. The introduced method has found to be performed better because of the resulted minimal distortion on the spectral characteristics. The authors have, also, found that the introduced method as to be very useful when implemented on vegetation analysis.

Mohanty and Majumdar (1997) [Moh 1997]: have attempted to unify the HIS with PAN images. The authors discovered a moderate spatial distortion in the HSI fused image.

Pohl and Van Gendren (1998) [Poh 1998]: provided a comprehensive review on image fusion techniques. Among those techniques, numerous HSI color transformation and Principal Component Analysis "PCA" techniques can be found that fused high resolution and medium resolution multi-spectral imageries.

Crawford *et al.* (1999) [Cra 1999]: Used data fusion of airborne polarimetric and interferometric SAR for classifying coastal environments. The polarimetric sensor measures the radar back-scatter from the surface and vegetation, which can be used to infer structural properties of the surface and their physical parameters. While data from interferometric sensor are, usually, used to determine the elevation of scatters within a resolution cell. Neural network classifier in a multi-resolution framework was utilized and a good accurately classified map of the coastal test site was obtained.

Li and Sheng (2000) [Li 2000]: described a fusion scheme based on wavelet transformation to fuse IR (Infra-Red) and visible images. They have reported that the spatial resolution of the IR is improved, and the salient detailed information for both the visible and the IR images were preserved.

Hameed Majeed Abdul Jabar(2006) [Jab 2006] Focused onto the two cases of satellite images fusion, multispectral-panchromatic and multiple panchromatic images fusion, by some transforms (wavelet and PCA) and some perceptual color spaces .

1.4 Book Layout

This book deals with satellite images fusion problem to produce more interpretive images, it is dispersed on five chapters, as given below

Chapter one

Presents a general introduction on remote sensing, showing the aim of this work, and a review for some of the related researches.

Chapter two

Presents the fundamental aspect of the remote sensing and image processing related to the satellite images and fusion problems. The adopted transformations; i.e. PCA, wavelet, and color transform for the fusion purposes have been investigated in some details.

Chapter three

In this chapter, the fundamental ideas for images fusion are presented. The fusion methods to unify multispectral image with panchromatic are illustrated in some details. The procedures followed to perform the PCA, Color, and Wavelet transformations are demonstrated. Image quality criteria are also given in this chapter.

Chapter four

The results of performing the adopted transformations are presented in this chapter. Tables showing the quantitative tests (i.e. presented in terms of NMSE, SNR, and the PSNR) between the resulted constructed images and the PAN images are demonstrated.

Chapter five

Specified to discuss the obtained results and concluding the superiority of each adopted fusion techniques on others. Several suggestions for future works are also proposed in this chapter.

CHAPTER TWO

Remote Sensing and Image Processing Principles

2.4 What is Remote Sensing

We perceive the surrounding world through our five senses. Some senses (touch and taste) require contact of our sensing organs with objects. However, we acquire much information about our surrounding through the senses of sight and hearing which do not require close contact between the sensing organs and the external objects. In another word, we are performing remote sensing all the time. Generally, remote sensing refers to:

1- The activities of recording, observing, perceiving (sensing) objects or events at faraway (remote) places. In remote sensing the sensors are not indirect contact with the objects or events being observed. The information needs a physical carrier to travel from the objects/events to the sensors through an intervening medium. The electromagnetic radiation is normally used as an information carrier in remote sensing [NRC 2007].

2- The science and technology, by which the characteristics of ground objects could be identified, measured or analyzed without physical direct contact with them. The devices, which detect the electromagnetic radiation (reflected or emitted from an object), are called "sensors", cameras and scanners etc., while a vehicle which carries the sensors is called "platform"; e.g. aircraft and satellites are examples of them [Azz 2001].

3-The science or / art of acquiring information about the Earth's surface without actually being in contact with it is called Remote Sensing. This is done by sensing and recording reflected or emitted energy and processing, analyzing, and applying that information.

There are a number of stages in a remote sensing process, each of them is important for successful operation; i.e.

- Emission of electromagnetic radiation, or EMR (sun/self- emission);
- Transmission of energy from the source to the surface of the earth, as well as absorption and scattering;
- Interaction of EMR with the Earth's surface: reflection and emission
- Transmission of energy from the surface to the remote sensor; and
- Sensor data output.

The mechanism of remote sensing in collecting data is illustrated in fig (2.1).

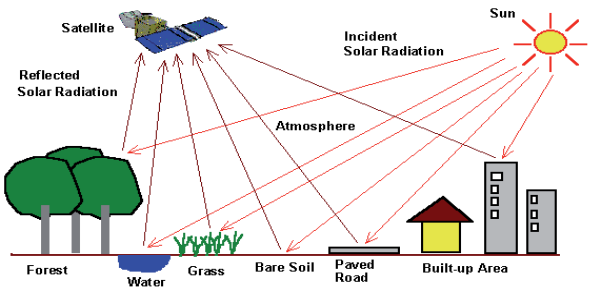

Figure (2.1) Remote sensing process [Lie 2001].

In most of remote sensing, the process involves interaction between incident radiation and the targets of interest; this is exemplified by the use of imaging systems which involve:

- ✓
- ✓ ***Energy Source of Illumination;***
- ✓ ***Radiation and the Atmosphere;***
- ✓ ***Interaction with Target;***
- ✓ ***Recording of Energy by the Sensor;***
- ✓ ***Transmission, Reception, and Processing;***
- ✓ ***Interpretation and analysis; and***
- ✓ ***Applications***

Note, moreover the remote sensing also involves the sensing of emitted energy and the use of non-imaging sensors.

2.2 The Electromagnetic Spectrum

The first requirement for remote sensing is to have an energy source to illuminate the target**;** otherwise the ***sensed energy is being emitted by the target***. This energy is in the form of electromagnetic radiation, which has fundamental properties and behaves in predictable ways according to the basics of the wave theory. ***Electromagnetic radiation*** consists of an ***electrical field (E)*** which varies perpendicularly with ***Magnetic field (M)*** along the radiation traveling path, both these fields travel at the speed of light (c).

The ***electromagnetic spectrum*** ranges from the shorter wavelengths (including gamma and x-rays) to the longer wavelengths (including microwaves and broadcast radio waves), shown in fig. (2.2). There are several regions of the electromagnetic spectrum which are useful for remote sensing. The ***electromagnetic spectrum*** is the continue of energy ranging from kilometers to nanometers in wavelength, traveling at $\cong 3\times10^{8}$ m/ sec, and capable of propagation through the space. All matter radiates a range of electromagnetic energy, with the peak intensity shifting toward progressively shorter wavelengths with increasing temperature [Sab 1978].

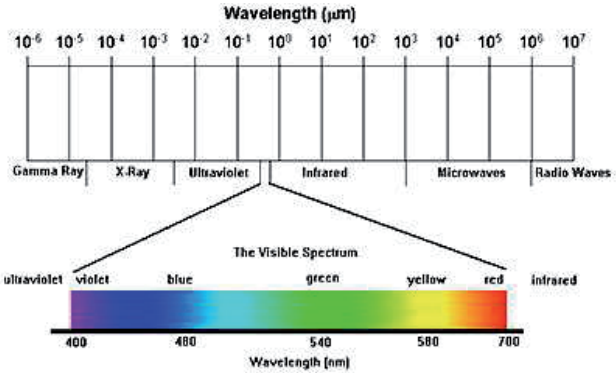

Figure (2.2): The Electromagnetic Spectrum [Lie 2001].

2.3 Type of Remote Sensing Imaging Resolutions

The conventional definition of resolution; is the ability to distinguish between two closely spaced objects on an image. This definition may be changed according of the type of resolutions it refer to; i.e. four types of resolution are encountered when dealing with remote sensing imaging; i.e.

2.3.1 Spatial Resolution and Pixel Size:

The spatial resolution of sensor refers to the size of the smallest possible feature that can be detected. The image resolution and pixel size are often used interchangeably. In reality, they are not equivalent; i.e. an image sampled at a small pixel size does not necessarily have higher resolution [NRC 2007, Nic 2007]. The following three images fig. (2.3) illustrate this point. The first image is a SPOT image of 10m pixel size; it was derived by merging a SPOT panchromatic image of 10m resolution with a

SPOT multispectral image of 20m resolution. The merging procedure colors the panchromatic image using the colors derived from the multispectral image.

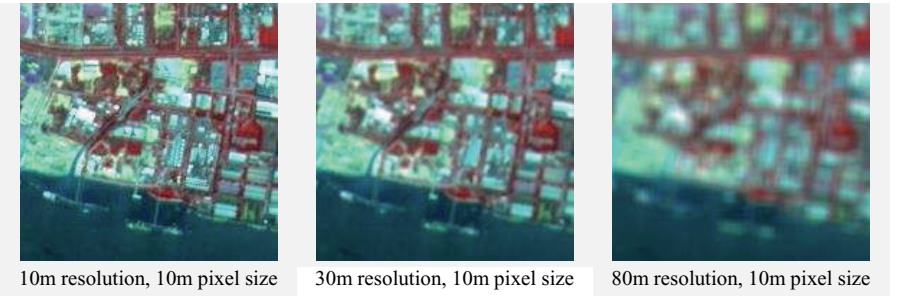

10m resolution, 10m pixel size | 30m resolution, 10m pixel size | 80m resolution, 10m pixel size

Figure (2.3): illustration of the difference between the resolution and the pixel's size [Lie 2001] .

The effective resolution is thus determined by the resolution of the panchromatic image, which is 10m. This image is further processed to degrade the resolution while maintaining the same pixel size. The next two images are the blurred versions of the image with larger resolution size, but still digitized at the same pixel size of 10 m. Even though they have the same pixel size as the first image, they do not have the same resolution. The following images fig. (2.4) illustrate the effect of pixel size on the visual appearance of an area.

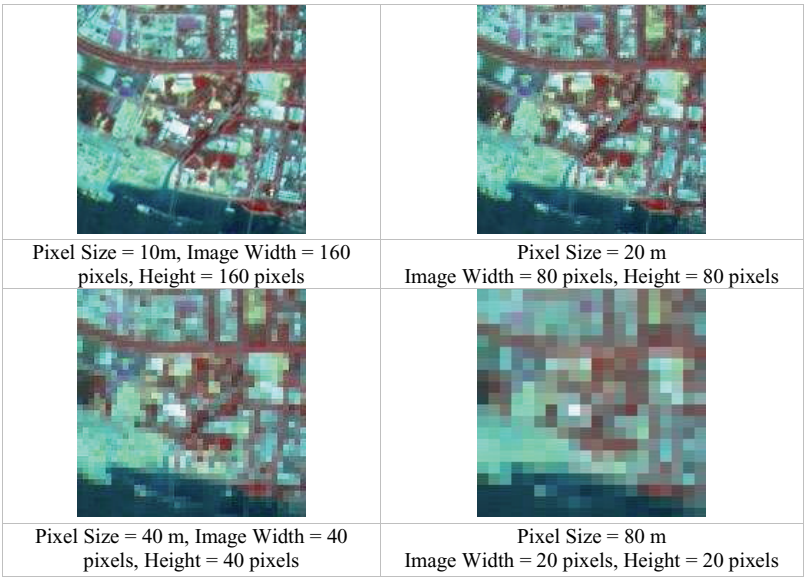

Pixel Size = 10m, Image Width = 160 pixels, Height = 160 pixels	Pixel Size = 20 m Image Width = 80 pixels, Height = 80 pixels
Pixel Size = 40 m, Image Width = 40 pixels, Height = 40 pixels	Pixel Size = 80 m Image Width = 20 pixels, Height = 20 pixels

Figure (2.4): Pixel size changed by averaging each four neighboring pixels [Lie 2001].

The spatial resolution sometimes expressed as the width of the ***instantaneous field of view (IFOV)*** (see fig (2.5)), or one side of a pixel (picture elements) [Jab 2006].

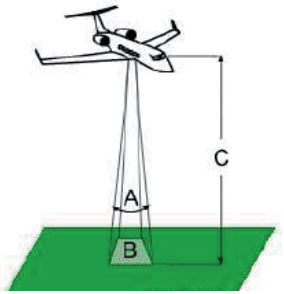

Figure (2.5): Instantaneous Field of View "IFOV" [NRC 2007].

The IFOV is the angular cone of visibility of the sensor (A) and determines the area on the Earth's surface which is "seen" from a given altitude at one particular moment in time (B). The size of the area viewed is determined by multiplying the IFOV by the distance from the ground to the sensor (c). The area on the ground is called the maximum spatial resolution of the sensor. So images where only large features are visible are said to have coarse or low resolution. The finer or high resolution images, small objects can be detected [NRC 2007].The spatial resolution of certain very commonly known satellite imagery is given in the table (2-1).

The military sensors are designed to view as much detail as possible therefore they have very fine resolution, while commercial satellites provide imagery with resolution varying from a few meters to several kilometers. Finally the finer the resolution, the less total ground area can be seen.

Table 2-1: Spatial resolution of certain well known satellites [RSN 1993].

Sensor	Spatial resolution in Multispectral mode [m]	Spatial resolution in Panchromatic [m]
IKONOS-2	4	1
LANDSAT-5	30	15
LANDSAT-7	28.5	14.25
SPOT 1,2,3	20	10
SPOT-5	10	5

2.3.2 Spectral Resolution

Different classes of features and details in an image can often be distinguished by comparing their responses over distinct wavelength ranges. Broad classes, such as water and vegetation, can usually be separated using very broad wavelength ranges (the visible and near infrared). Other more specific classes, such as different rock type, may not be easily distinguishable by using the broad wavelength ranges and would require a sensor with higher spectral resolution. Spectral resolutions describe the ability of the sensor to define fine wavelength intervals and it's defined as the width within the electromagnetic spectrum can be detected by a band of sensor [NRC 2007, Jab 2006].

The spectral resolutions achieved by a sensor depends on the number of bands, there bandwidths, and there location within the electromagnetic spectrum. Fig (2.6) gives example on spectral bands of "TM" on Landsat [Sho 2007, Moo].

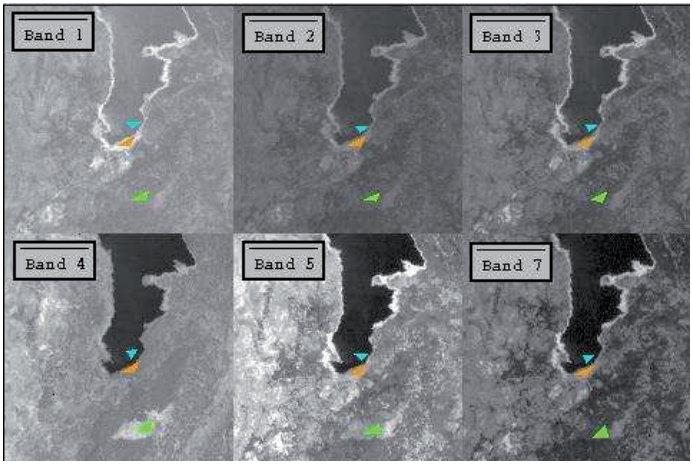

Figure (2.6): LandSat TM bands 1, 2, 3, 4, 5, and 7 [Moo].

Spectral properties of the data provide by some well known satellites are presented in table (2-2).

Table 2-2: Spectral Resolutions for Some Common Sensors [Moo]	
Remote Sensing Instrument	**Spectral Bands (in micrometers)**
Landsat TM (Thematic Mapper)	1. 0.45 - 0.52 (Blue) 2. 0.52 - 0.60 (Green) 3. 0.63 - 0.69 (Red) 4. 0.76 - 0.90 (Near-Infrared) 5. 1.55 - 1.75 (Middle-Infrared) 6. 10.4 - 12.5 (Thermal) 7. 2.08 - 2.35 (Middle-Infrared)
Landsat ETM+ (Enhanced Thematic Mapper Plus)	Above TM bands Plus 0.50-0.90 (Panchromatic)
Landsat MSS (Multispectral Scanner)	4. 0.5 - 0.6 (Green) 5. 0.6 - 0.7 (Red) 6. 0.7 - 0.8 (Near-Infrared) 7. 0.8 - 1.1 (Near-Infrared) 8. 10.4 - 12.6 (Thermal)
SPOT HRV (High Resolution Visible)	1. 0.50 - 0.59 (Green) 2. 0.61 - 0.68 (Red) 3. 0.79 - 0.89 (Near-Infrared) 4. 0.51 - 0.73 (Panchromatic)

2.3.3 Radiometric Resolution

While the arrangement of pixels describes the spatial structure of the image, the radiometric characteristics describe the actual information content in the image. Every time an image is acquired on film or by a sensor, its sensitivity to the magnitude of the electromagnetic energy determines the **radiometric resolution**. The radiometric resolution of an imaging system describes its ability to discriminate very slight differences in energy, the finer the radiometric resolution of a sensor the more sensitive it is to detecting small differences in reflected or emitted energy. Fig. (2.7) illustrates the differences between six scenes having different radiometric resolution [NRC 2007].

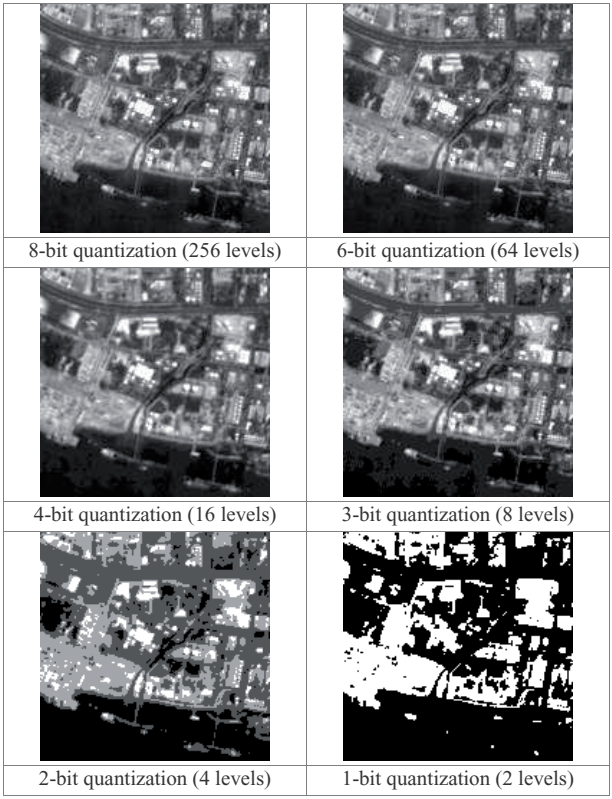

Figure (2.7): Illustration the difference between six different radiometric resolution scenes [NRC 2007].

Imagery data are represented by positive digital numbers which vary from 0 to (one less than) a selected power of 2. This range corresponds to the number of bits used for coding numbers in binary format. The maximum number of brightness levels available depends on the number of bits used in representing the energy recorded. Thus, if a sensor used 8 bits to record the data, there would be 2^8=256 digital values available, ranging from 0 to 255.

2.3.4 Temporal Resolution

Temporal resolution refers to the precision of measurement with respect to time. There is a trade-off between temporal resolution and its spatial resolution. The concept of **temporal resolution** is important in a remote sensing system. The absolute temporal resolution of a remote sensing system to image for the exact same area at the same viewing angle a second time is equal to this period. Thus, the actual temporal

resolution of a sensor depends on a variety of factors, including the satellite/sensor capabilities, the swath overlap, and latitude [NRC 2007].

The ability to collect imagery of the same area of the Earth's surface at different periods of time is one of the most important elements for applying the remote sensing data. Spectral characteristics of features may change over time and these changes can be detected by collecting and comparing **multi-temporal** imagery. For example, during the growing season, most species of vegetation are in a continual state of change and our ability to monitor those subtle changes using remote sensing is dependent on when and how frequently we collect imagery. By imaging on a continuing basis at different times we are able to monitor the changes that take place on the Earth's surface, whether they are naturally occurring (such as changes in natural vegetation cover or flooding) or induced by humans (such as urban development or deforestation).

So the time factor in imaging is important when:

- Persistent clouds offer limited clear views of the Earth's surface (often in the tropics);
- Short-lived phenomena (floods, oil slicks, etc.) need to be imaged;
- Multi-temporal comparisons are required (e.g. the spread of a forest disease from one year to the next); and
- The changing appearance of a feature over time can be used to distinguish it from near similar features (wheat / maize).

2.4 Satellites

Satellite is an artificial object constructed by humans revolve around another object and placed in orbit around the earth or other celestial body. For example the Moon is a natural satellite, whereas man-made satellite includes those platforms lunched for remote sensing, communication, and telemetry (location and navigation) purpose. The satellite is lifted from the earth's surface by a rocket and, once placed in orbit, maintains its motion without further rocket propulsion. The first artificial satellite, *Sputnik I,* (shown in fig. (2.8)), was launched on Oct. 4, 1957, by the USSR; a test payload of a radio beacon and a thermometer demonstrated the feasibility of orbiting a satellite.

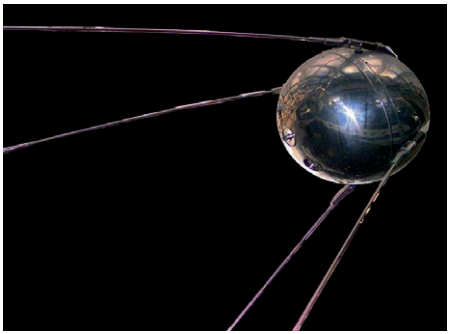

Figure (2.8): The first artificial satellite (Sputnik I) launchedon Oct. 4, 1957[Wik].

The first U.S. satellite, shown in fig. (2.9), *Explorer I* launched on Jan. 31, 1958, returned data that was instrumental in the discovery of the Van Allen radiation belts. During the first decade of space exploration, all of the satellites were launched from either the United States or USSR. Examples of some well-known working satellite are shown in fig. (2.10).

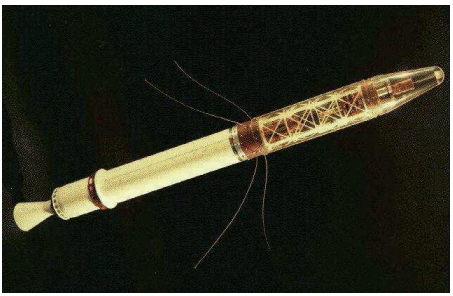

Figure (2.9): The first U.S. satellite, Explorer I, launched on Jan. 31, 1958 [wik].

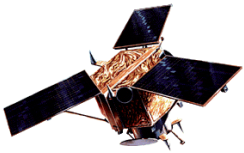

IKONOS 2

SPOT

EROS A1

LANDSAT 7

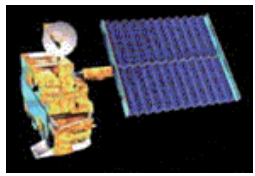

TERRA

NOAA 12, 14, 16

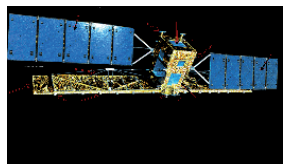

RADARSAT 1

Figure (2.10): Example of Some Well-Known satellites [Lie 2001].

There are three basic categories of non-military satellite services [Gra 2004]:

- ***Fixed Satellite Service***: handle hundreds of billions of voice, data, and video transmission tasks across all countries and continents between certain points on the earth's surface;
- ***Mobile Satellite Systems***: help connect remote regions, vehicles, ships and aircraft to other parts of the world and/or other mobile or stationary communications units, in addition to serving as navigation systems.
- ***Scientific Research Satellite (commercial and noncommercial)***: Scientific research satellites provide us with meteorological information, land survey data (e.g., remote sensing), and other different scientific research applications such

as earth science, marine science, and atmospheric research.

Satellites can be categorized according to their jobs; i.e.

- Anti-Satellite weapons/"Killer Satellites": they are satellites that are armed, designed to take out enemy warheads, satellites, other space assets. They may have particle weapons, energy weapons, kinetic weapons, nuclear and/or conventional missiles and/or a combination of these weapons.
- ***Astronomical satellites:*** they are satellites used for observation of distant planets, galaxies, and other outer space objects.
- ***Biosatellites:*** they are satellites designed to carry living organisms, generally for scientific experimentation.
- ***Communications satellites:*** they are satellites stationed in space for the purpose of telecommunications. Modern communications satellites typically use geosynchronous orbits, Molniya orbits or Low Earth orbits.
- ***Miniaturized satellites:*** they are satellites of unusually low weights and small sizes. New classifications are used to categorize these satellites: mini-satellite (500–200 kg), microsatellite (below 200 kg), nano-satellite (below 10 kg).
- ***Navigational satellites:*** they are satellites which use radio time signals transmitted to enable mobile receivers on the ground to determine their exact location. The relatively clear line of sight between the satellites and receivers on the ground, combined with ever-improving electronics, allows satellite navigation systems to measure location to accuracies on the order of a few meters in real time.
- ***Reconnaissance satellites:*** they are Earth observation satellite or communications satellite deployed for military or intelligence applications. Little is known about the full power of these satellites, as governments who operate them usually keep information pertaining to their reconnaissance satellites classified.
- ***Earth observation satellites:*** they are satellites intended for non-military uses such as environmental monitoring, meteorology, map making etc.
- ***Space stations:*** they are man-made structures that are designed for human beings to live on in outer space. A space station is distinguished from other manned spacecraft by its lack of major propulsion or landing facilities instead, other vehicles are used as transport to and from the station. Space stations are designed for medium-term living in orbit, for periods of weeks, months, or even years.

- ***Tether satellites:*** they are satellites which are connected to another satellite by a thin cable called a tether.
- ***Weather satellites:*** they are primarily used to monitor Earth's weather and climate.

Satellite's Orbit Types: ***They can be classified according to their orbits;***

1. Orbit's heights:
   - Low Earth Orbit (LEO): is any orbit below 2000 km;
   - Medium Earth Orbit (MEO): is any orbit higher than that but still below the altitude for geosynchronous orbit at 35786 km;
   - High Earth Orbit (HEO): is any orbit higher than the altitude for geosynchronous orbit.
   - Orbit's Inclination: inclination reference to the equatorial plane is not zero degrees:
   - Polar orbit: An orbit that passes above or nearly above both poles of the planet on each revolution. Therefore it has an inclination of (or very close to) 90 degrees.
   - Polar sun synchronous orbit: A nearly polar orbit that passes the equator at the same local time on every pass. Useful for image taking satellites because shadows will be nearly the same on every pass.

There are many other classification of the satellite, can be seen in the literature, for instance see [Wik].

2.5 Scientific Remote Sensing Satellites:

Today, several nations operate or plane to operate remote sensing satellite, specifically designed for observation of earth resources, including crops, forests, water bodies, land use, and minerals. Satellite sensors offer several advantages over aerial photography; they provide a synoptic view (observation of large areas in a single image), as well as find details and systematic, repetitive coverage. Such capabilities are well suited to creating and maintaining a worldwide cartographic infrastructure and to monitoring many of the broad-scale environmental problems that the world faces today [Cam 1996].

Several remote sensing satellites are currently available, providing imagery suitable for various types of applications. Each of these satellite-sensor platforms is characterized by the ***wavelength bands*** employed in image acquisition, ***spatial resolution*** of the sensor, the ***coverage area*** and the ***temporal coverage (***i.e. how

frequent a given location on the earth surface can be imaged by the imaging system).
In terms of the spatial resolution, the satellite imaging systems can be classified into:

- Low resolution systems (approx. 1 km or more/pixel)
- Medium resolution systems (approx. 100 m to 1 km/pixel)
- High resolution systems (approx. 5 m to 100 m/pixel)
- Very high resolution systems (approx. 5 m or less/pixel)

In terms of the spectral regions used in data acquisition, the satellite imaging systems can be classified into:

- Optical imaging systems (include visible, near infrared, and short-wave infrared systems).
- Thermal imaging systems.
- Synthetic aperture radar (SAR) imaging systems.

Optical/thermal imaging systems can be classified according to the number of spectral bands used:

- Monospectral or panchromatic (single wavelength band, "black-and-white", gray-scale image) systems
- Multispectral (several spectral bands) systems
- Superspectral (tens of spectral bands) systems
- Hyperspectral (hundreds of spectral bands) systems [Lie 2001].

2.5.1 LANDSAT:

The Landsat program consists of a series of optical/infrared remote sensing satellites for land observation. The program was first started by the National Aeronautics and Space Administration (NASA) in 1972, then turned over to the National Oceanic and Atmospheric Administration (NOAA) after it became operational. Since 1984, satellite operation and data handling were managed by a commercial company EOSAT. However, all data older than 2 years return to "public domain" and are distributed by the Earth Resource Observation System (EROS) Data Center of the US Geological Servey (USGS).

The first satellite in the series, Landsat-1 (initially named as the Earth Resource Technology Satellite ERTS-1) was launched on 23 July 1972. The satellite had a designed life expectancy of 1 year, but it ceased operation only on January 1978. Landsat-2 was launched on 22 January 1975 and three additional Landsat satellites were launched in 1978, 1982, and 1984 (Landsat-3, 4, and 5 respectively). Landsat-6 was launched on October 1993 but the satellite failed to attain the orbit. A new satellite Landsat-7 was launched in 15 April 1999. Currently, only Landsat-5 and 7 are operational [Jab 2006].

The sensors carried on-board Landsat series are the following

1. MSS (Multi-Spectral Scanner), on Landsat-1 to 5. The resolution of the MSS sensor was approximately 80 m with radiometric coverage in four spectral bands from the visible green to the near-infrared (IR) wavelengths. Only the MSS sensor on Landsat 3 had a fifth band in the thermal-IR.
2. TM (Thematic Mapper), its first operation was on Landsat-4. TM sensors primarily detect reflected radiation from the Earth surface in the visible and near-infrared (IR) wavelengths, but the TM sensor provides more radiometric information than the MSS sensor. The TM sensor has a spatial resolution of 30 m for the visible, near-IR, and mid-IR wavelengths and a spatial resolution of 120 m for the thermal-IR band.
3. ETM+ (Enhanced Thematic Mapper Plus) is carried on board Landsat 7. The ETM+ instrument is an eight-band multispectral scanning radiometer capable of providing high-resolution image information of the Earths surface. Its spectral bands are similar to those of TM, except that the thermal band (band 6) has an improved resolution of 60 m (versus 120 m in TM). Also there is an additional panchromatic band at 15 m resolution.

2.5.2 SPOT

SPOT (Satellite Pour l'Observation de la Terre) is a high-resolution, optical imaging earth observation satellite system operating from space. It is run by SPOT Image based in Toulouse, France. It was initiated by the CNES (Centre national d'études spatiales – the French space agency) in the 1970s and was developed in association with the SSTC (Belgian scientific, technical and cultural services) and the Swedish National Space Board (SNSB). It has been designed to improve the knowledge and management of the earth by exploring the earth's resources, detecting and forecasting phenomena involving climatology and oceanography, and monitoring human activities and natural phenomena. The SPOT system includes a series of satellites and ground control resources for satellite control and programming, image production, and distribution. The satellites were launched with the ESA rocket launcher Ariane 2, 3, and 4. The SPOT orbit is polar, circular, sun-synchronous, and phased. The inclination of the orbital plane combined with the rotation of the earth around the polar axis allows the satellite to fly over any point on earth within 26 days [Wik 2008].

The company SPOT Image is marketing the high-resolution images, which SPOT can take from every corner of the earth.[Wik 2008]

- SPOT-1 launched on February 22, 1986 with 10m panchromatic and 20m

multispectral picture resolution capability. Withdrawn December 31, 1990.

- SPOT-2 launched on January 22, 1990 and is still operational.
- SPOT-3 launched on September 26, 1993.
- SPOT-4 launched on March 24, 1998
- SPOT 5 launched on May 4, 2002 with 2.5m, 5m and 10m apability

2.6 Multispectral Images

Multispectral images typically contain information outside the normal human perceptual range. This may include infrared, ultraviolet, X-ray, acoustic, or radar data. These are not images in the usual sense because the information represented is not directly visible by the human system. However, the information is often represented in visual form by mapping the different spectral band to the RGB components. If more than three bands of information are in the multispectral image, dimensionality is reduced by applying a Principal Component Transform (PCT) [Umb 1998]. Sources of these types of images include under water sensor systems, varies types of airborne radar, infrared imaging systems, medical diagnostic imaging system and satellite systems [Umb 1998].

2.7 Panchromatic Images

A Panchromatic Images consist of only one band and it is usually displayed as gray-scale image. It referred to as monochromatic, or one – color image; i.e. contains brightness information only. The number of bits used for each pixel determines the number of different brightness level available. The typical image contains 8 bit/pixel data, which allows having 256 (0-255) different brightness (gray) levels [Umb 1998].

2.8 Resampling and Quantization Methods

The treatments of resampling and quantization often utilize to zoom and shrink digital images. ***Zooming*** may be viewed as over sampling, while ***Shrinking*** may be viewed as under sampling. ***Zooming*** requires two steps: the creation of new pixel locations, and the assignment of gray levels to those new locations. Image shrinking is performed in a similar manner as for zooming. The equivalent process of pixel replication is row-column deletion. For example, to shrink an image by one-half, we delete every other row and column. We can use the zooming grid analogy to visualize the concept of shrinking by a noninteger factor. For instance, to double the size of an image, we can duplicate each column. This doubles the image size in the horizontal direction. Then, we duplicate each row of the enlarged image to double the size in the vertical direction. The same procedure is used to enlarge the image by any integer number of times (triple, quadruple, and so on). Duplication is just done the required

number of times to achieve the desired size. The gray-level assignment of each pixel should be predetermined by the fact that new locations are exact duplicates of old locations. Determining the gray level of the interpolated pixel may be carried by different ways; i.e.

2.8.1 Nearest Neighbor

Nearest-neighbor interpolation (also known as proximal interpolation or point sampling in some contexts) is a simple method of multivariate interpolation in one or more dimensions. Interpolation is the problem of approximating the value for a non-given point in some space, when given some values of points around that point. The nearest neighbor approach uses the value of the closest input pixel for the output pixel value, and does not consider the values of other neighboring points at all, yielding a piecewise-constant interpolant. The algorithm is very simple to implement, and is commonly used to select color values for a textured surface.

As illustrated in fig (2.11.a), the nearest point is determined according the following equation [Azz 2001]:

$$\begin{aligned} &Q(u,v) = P_{KI} \\ &K = \lfloor u + 0.5 \rfloor \\ &I = \lfloor v + 0.5 \rfloor \end{aligned} \quad , \qquad \text{..... (2.1)}$$

Where, $Q(u,v)$: A point to be interpolated

P_{ij}: Input image data

[ ]: Gaussian symbol to make integer

$s = u - \lfloor u \rfloor \quad , \quad t = v - \lfloor v \rfloor$

2.8.2 Bilinear Interpolation

In this method, the value of the rectified pixel is based upon the distance between the transformed coordinate location and the four closest pixels in the input image. Bilinear determines the gray level from the weighted average of the four closest pixels to the specified input coordinates and assigns that value to the output coordinates. It generates an image appearance smoother than Nearest Neighbor, but the gray level values are resulting in blurring or loss of image resolution [Aub 2007].

As shown in fig. (2.11.b), this interpolation method can be described by the following equation:

$$Q(u,v) = (1-s)(1-t)P_{ij} - (1-s)tP_{ij+1} + s(1-t)P_{i+1j} + stP_{i+1j+1} \qquad \text{..... (2.2)}$$

2.8.3 Cubic Convolution Interpolation

Cubic convolution is the name of an interpolation method using two cubic polynomials to define the weighting coefficients for the four surrounding points (in one-dimension), two to the left and two to the right as shown in fig. (2.11.c). The interpolation by this method can be performed by using 16 points (in two-dimension), which surrounded each output pixel. The appearance of the resultant image is more acceptable comparing with other methods, but the disadvantage of these methods lies in its complexity. However this method is performed by, [Azz 2001]

$$Q(u,v) = \left[f(1+t)\,f(t)\,f(1-t)\,f(2-t)\right]\begin{bmatrix} P_{11} & P_{12} & P_{13} & P_{14} \\ P_{21} & P_{22} & P_{23} & P_{24} \\ P_{31} & P_{32} & P_{33} & P_{34} \\ P_{41} & P_{42} & P_{43} & P_{44} \end{bmatrix}\begin{bmatrix} f(1+s) \\ f(s) \\ f(1-s) \\ f(2-s) \end{bmatrix} \quad \ldots (2.3)$$

Let,

$$f(x) = \sin(\pi x)/(\pi x) \qquad , \ldots\ldots\ldots\ldots (2.4)$$

$$= \begin{cases} 1-2|x|^2+|x|^3 & (0 \le |x| < 1) \\ 4-8|x|+5|x|^2-|x|^3 & (0 \le |x| < 2) \\ 0 & (2 \le |x|) \end{cases} \qquad , \ldots\ldots\ldots\ldots\ldots (2.5)$$

Then,

$$\begin{aligned} f(1+y) &= -y(1-y)^2 \\ f(1-y) &= y + y^2(1-y) \\ f(y) &= (1-y) + y(1-y)^2 \\ f(2-y) &= -y^2(1-y) \end{aligned} \qquad , \ldots\ldots\ldots\ldots\ldots (2.6)$$

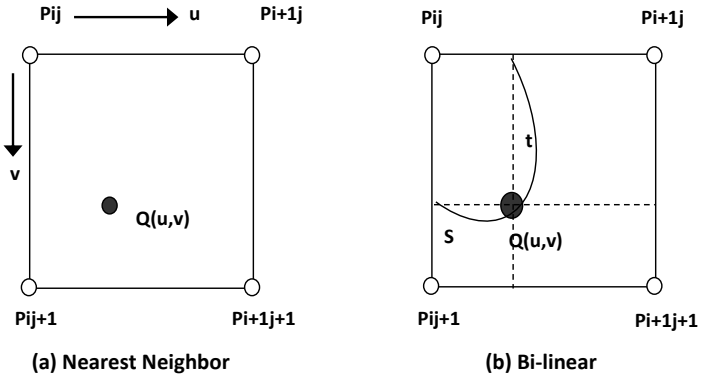

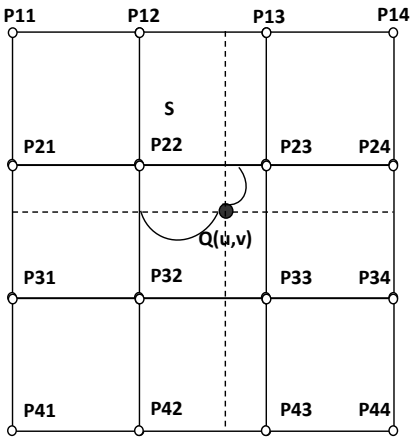

Figure (2.11): a, b, and c representing different 2D- interpolation techniques, [Azz 2001]

2.9 Image Transformations

Image transformations generate "new" images from sources which highlight. Particular features or properties of interest, better than the original input images, by applying Basic simple arithmetic operations to the image data (sources).

Transform Theory has played a key in image processing for a number of years, and it continues to be a topic of interest in theoretical as well as applied work in this field [Gon 1977].

2.9.1 Principal Components Transform (PCT)

Principal Component analysis is one of the oldest techniques that are used in multivariate analysis. It was introduced by *Pearson* (1901) in order to recast linear regression analysis into a new form. It was then developed by *Hotelling* (1933) in work done on psychometric. *Karhunen* (1947) used it in the setting of the probability theory, and was subsequently generalized with *Loeve* (1948). The Principal Components transform was introduced as a series expansion for continuous random process by Karhunen and Loeve. For random sequences Hotelling (1933) first studied what was called a method of principal components, which is the discrete representation equivalent of the Karhunen-Loeve series expansion. Consequently, the Principal Component (PC) transform is also called the Hotelling, eigenvector, or Karhunen-Loeve (KL) transformation [Shm 1999].

The *principal component* analysis or *Karhunen-Loeve* transform is a mathematical way of determining that linear transformation of a sample of points in N-dimensional space which exhibits the properties of the sample most clearly aligned along the coordinate axes. Along the new axes the sample variances are extremes (maxima and minima), and uncorrelated. The name comes from the *principal axes* of an ellipsoid (e.g. the ellipsoid of inertia), which are just the coordinate axes in question [Jab 2006].

So the effect of computing the principal components of a distribution is to determine a new set of axes with two related properties:

1. The axes may be ordered by their "information content". Thus using only the first axis, the best one dimensional representation of the data is obtained, by using the first two; the best two dimensional representation is obtained, and so on.
2. The data expressed in the new axes are uncorrelated [Nib 1986].

An interesting application of *principle component* analysis is in the detection of features that change with time between images of the same region [Rec 1998], and another interesting application is in the data compression. It allows redundant data to be compacted into fewer bands that is; the dimensionality of the data is reduced. The bands of PCA data are uncorrelated and independent, and are often more interpretable than the source data [Jen 1996, Fau 1989].

2.9.1.1 Properties of the (PCT)

The PCT has several interesting properties, which can be summarized as follows:

- It is a rigid rotation of the original coordinate axes such that there is coincidence with the major axes between two spaces. The data in the PC image result from projecting the original data onto the new axes. Some of PC's (higher than first) could take negative values; this problem is easily overcome by shifting, such that all PC's values will be in the positive range without changing the mathematical behavior of the original PC's.
- The resultant PC's are orthogonal to each other, so each component represents a unique feature of the multi -band image. This property could be successfully utilized in the classification and compression of the images.
- They redistribute the total image variance with optimum manner. The first **(*PC*)** image contains the maximum amount of variance for any linear combinations of the original bands, while the second ***(PC)*** image contains the maximum possible variance for any axis orthogonal to the first **(*PC)***, and so forth. Thus all the PC's will preserve the total image variance.
- The calculated eigenvalues and eigenvector matrix are highly data dependent. To interpret the PC's, one must already has some priory knowledge about the overall interpretation of the original data [Azz 2001].

2.9.1.2 The (PCT) Analysis

Groups of images of the same scene but differing in spectral properties are known as bands. The ensemble of bands is known as a ***multi-band*** **or** ***multi-spectral*** image .If a scene has *m* bands, the PCT of the images will also have *m* bands.

However, the bands of transforming multi-spectral image are ordered in terms of their information content. The first PC-band has the largest information content, the second the next largest and so on. The later PC-band may contain so little information that visually they resemble noise. The storage saving comes from discarding these low information content bands. The principal component transform can be written as a vector equation given by [Azz 2001];

$$P = H\,(b - m) \quad , \ldots\ldots\ldots\ldots\ldots (2.7)$$

In this equation P is the transformed vector, H is the transformation matrix, b is the original vector and *m* is vector representing the expectation value of b. Equation (2.7), shows how to transform our original data in b to the result in P. The vector b represents the set of pixel values in each band at a given position.

Principal Component analysis allows us to remove correlation between the bands of-multi-spectral images. This technique can be used to reduce the amount of

data needed to represent a particular set of images. The removal of redundant information has the obvious practical effect of reducing the amount of storage requires to hold the data. It is also useful precursor to image classification [Lia 1990].

2.9.2 Wavelet Transformation

Multiresolution decomposition provides a simple hierarchical framework to analysis images with different spatial resolution. It is a powerful tool to separate the spectral content of an image from the spatial information [Bre 2000].

The wavelet transform is really a family of transforms that satisfy specific conditions. And it is probably the most recent solution to overcome the shortcomings of the Fourier Transform. From our perspective, the *wavelet transform* can be described as a transform that has basis functions that are shifted aim expanded versions of themselves. Because of this, the wavelet transform contains not just frequency information but spatial information as well. One of the most common models for a wavelet transform uses the Fourier transform and high-pass and low-pass filters. To satisfy the conditions for a wavelet transform, the filters must be *perfect reconstruction filters,* which mean that any distortion introduced by the forward transform will be canceled in the inverse transform [San 2001] [Umb 1998].

The Multiresolution wavelet transform has been applied to signal processing and image processing in various ways. In particular, it has been widely used for image compression, boundary extraction, object recognition and image fusion in image processing [Kan 2001, Gar 1996].

The wavelet transform breaks an image down into four sub-sampled or decimated images. They are sub-sampled by keeping every other pixel. The results consist of one image that has been high-pass filtered in both the horizontal and vertical directions, one that has been high-pass filtered in the vertical and low-pass filtered in the horizontal, one that has been low-passed in the vertical and high-passed in the horizontal, and one that has been low-pass filtered in both directions [Umb 1998].

The transform is typically implemented in the spatial domain by using 1-D convolution filters. Since the wavelet transform basis functions are separable, one can perform the 2-D transform by using two 1-D transforms. In order to perform the wavelet transform with convolution filters, a special type of convolution called circular convolution must be used. Circular convolution is performed by taking the underlying image array and extending it in a periodic manner to match the symmetry implied by the discrete Fourier transform [Jab 2006].

2.9.2.1 Continuous Wavelet Transform (CWT)

The CWT is the sum over the whole time of the signal multiplied by scaled and shifted versions of the wavelet function ψ. The process produces wavelets coefficients that are a function of scale and position can be written as; [Are 2003, Sta 1998]

$$w(a,b) = \frac{1}{\sqrt{a}} \int_{-\infty}^{\infty} f(x)\psi(\frac{x-b}{a})dx \qquad \text{, ... (2.8)}$$

Where: *W (a,b)* the wavelet coefficient of the function *f(x).*

ψ(x) the analyzing wavelet

a (>0) the scale parameter

b the position parameter

Scaling a wavelet means stretching (or compressing) it. It is done by keeping the shape while changing the one-dimensional time scale a (a>0).

$$\frac{1}{\sqrt{a}}\psi(\frac{x}{a})$$

Shifting a wavelet simply means delaying its onset. In other words, move the basic shape form one side to the other. Translating to position *b*.

$$\psi(x-b)$$

2.9.2.2 Discrete Wavelet Transform (DWT)

Information provided by continues wavelet transform (CWT) is highly redundant as far as the reconstruction of the signal or image is required. DWT provides information enough for analysis and synthesis with an important reduction of computation time [Are 2003]. Information that comes from signal or image we deal with it (analyzed or processed) are in discrete form recall that the CWT (Equation 2.8) is the integral of the product $f(x)\psi(\frac{x-b}{a})$. The corresponding calculation for the discrete case (the DWT) involves a convolution, but experience show that the quality of this type of transform depends heavily on two things the choice of scale factors and time shifts, and the choice of wavelet [Sal 2004].

For processing classical signals (i.e. regularly pixilated) sampling is carried out in accordance with Shannon's well known theorem. The discrete wavelet transform (DWT) can be derived from this theorem if we process a signal which has a cut-off frequency. If we are considering images, we can note that the frequency band is always limited by the size of the camera aperture [Sta 1998]. In practice, the DWT is computed with scale factors that are negative of 2 and time shifts that are non-

negative powers of 2. Fig. (2.12) shows the so-called dyadic lattice that illustrates this particular choice [Sal 2004].

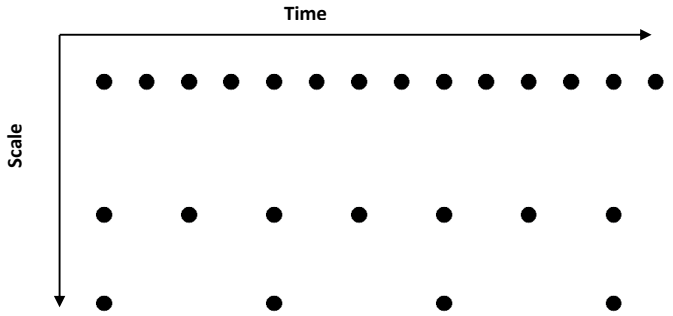

Figure (2.12): The Dyadic Lattice showing the relationship between the scale factor and Time, [Sal 2004].

The mean that we increase the scale and step spacing between wavelets by factor of two at each step, e.g., the first pass, we would use wavelets of scale, and space them, sample apart. Then the second pass, we'd scale them to two samples, and space them apart by two sample points.

What we do is taking a low-pass (scaling function) and a high-pass (wavelet function) version of the curve and separates the high-pass information. In short, we treat the wavelet transformation as if it is a filter bank. And we iterate downward along the low-pass sub-band. The low-pass data is treated as a signal in its own right and is subdivided in its own low and high sub-bands.

Ultimately, we can go all the way down until the low-pass and high-pass bands are a single value, but whether or not we do that depends on the application.

2.9.2.3 One-Dimensional DWT Algorithms

A) 1-D Decomposition steps:

For any input signal 'S', the discrete wavelet transform "*DWT*" is performed as illustrated in fig. (2.13); i.e.

The first step produces two sets of coefficients; i.e. approximation coefficients, and detail coefficients. These vectors are obtained by convolving with a low-pass filter, and a high-pass filter, respectively. Then followed by dyadic decimation, [MAT6.5].

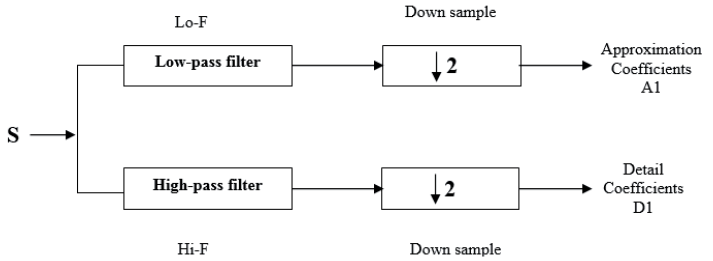

Figure (2.13) Signal Decomposition step [MAT6.5]

The next step splits the approximation coefficients in two parts, using the same above scheme, replacing (S) by the approximation coefficients (A_j, where the subscript "j" represents the transformation levels). The wavelet decomposition of the signal "S" is, thus, analyzed at any levels "j", following tree structures, shown in fig. (2.14).

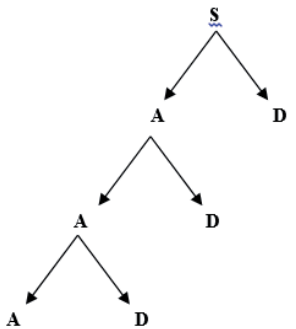

Figure (2.14): Signal Decomposition Structure, fort j=3, **[MAT 6.5].**

B) 1-D Reconstruction Steps:

Conversely, the inverse wavelet transformation should start from A_j and D_j, reconstructing, recursively A_{j-1}. In fact, inverse transformation applying the same decomposition steps but, by inserting zeros in the empty rows or columns, then convoluting the results with the reconstruction filters, illustrated in fig. (2.15).

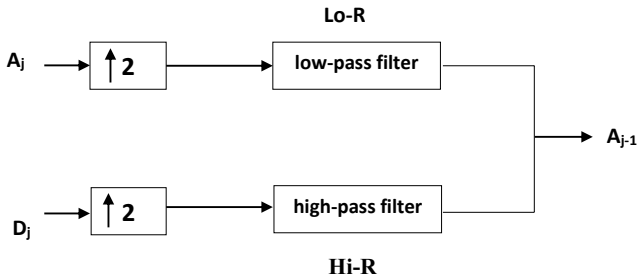

Figure (2.15): DWT reconstruction operations [MAT 6.5].

2.9.2.4 Two-Dimensional Image DWT Algorithms

A) 2D image Decomposition steps:

The low-pass and high-pass wavelet filters used for decomposition. The rows of the image are convolved with the low-pass and high-pass filters and the result is down sampled along the columns. This yields two sub-images whose horizontal resolutions are reduced by a factor 2. The high-pass or detailed coefficients characterize the image's high frequency information with vertical orientation while the low-pass component contains its low frequency, vertical information. Both sub-images are again filtered column wise with the same low-pass and high-pass filters and down-sampled along rows. This process results four sub-images each reduced by a factor of four compared to the original image, fig. (2.16), [MAT6.5].

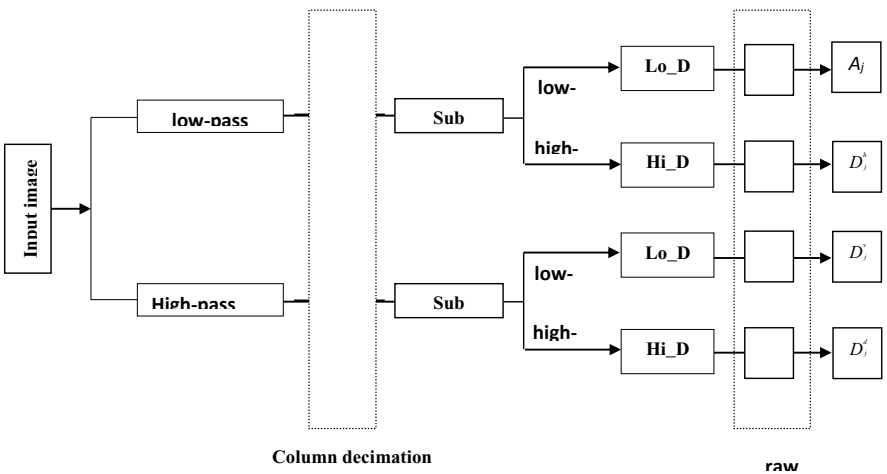

Figure (2.16): 2D Image Decomposition Steps [ERD 8.7]

The 2D- DWT leads to decomposition of image in four components: the approximation at level j and the details in three orientations (horizontal, vertical, and diagonal), as follows:

Approximation coefficients A_j,

horizontal coefficients D_j^h - variations along the columns.

Vertical coefficients D_j^v - variations along the rows.

Diagonal coefficients D_j^d - variations along the diagonals.

B) 2D image Reconstruction Steps:

The reduced components of the input images are passed as input to low-pass and high-pass reconstruction filters, as shown in fig. (2.17).

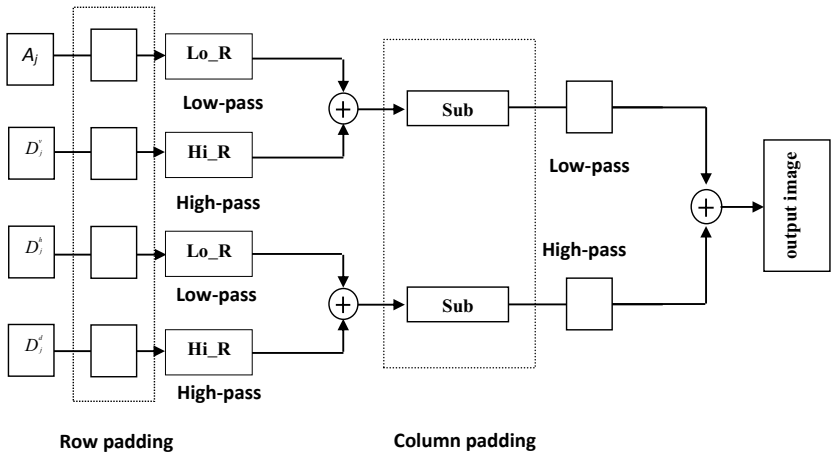

Figure (2.17): 2D – Reconstruction Steps [ERD 8.7]

The sequence of steps is the opposite of that in the DWT, the sub-images are up-sampled along rows and convolved with low-pass and the high-pass filters column-wise. These intermediate output are like in sequences. Up-sampled along columns and then filtered row-wise and finally concatenated to yield the original images [MAT6.5].

2.10 Color Space

There are many definitions for the color space, but in general they agree to some extent in their description to the color space (as a model to represent the colors in terms of numbers).

To illustrate this agreement, some definitions are presented below:-

*A color spaces lend themselves in principle to reproducible representation of color, particularly in digital representations (i.e. digital printing or digital electronic display). [Wik 2005]

*A color space is coordinate system designed to allow colors to be measured and quantitatively specific [Nib1986].

*A color space is a model for representing color in terms of intensity values; a color space specific how color information is represented. It defines a one-two-three-or four-dimensional space whose dimensions or components represent intensity values. From tristimulus color theory, a three dimensional space is necessary, but various choices for the three coordinates are possible. Three general forms of color space coordinates are: - [Nib 1986]

1. Tristimulus coordinates: A rectangular space in which the three coordinates, called the tristimulus values, give the amount of each of three fixed primaries. The recommended sets of primaries are the CIE (commission international d'Eclairage) 1931 XYZ primaries, but other sets may be used. It is customary to set the scale factor so that (1, 1, 1) gives a reference white.
2. Chromaticity coordinates: (x,y) coordinates derived from tristimulus coordinates (X,Y,Z) as described previously. To fully specify a color, its luminance must be specified in addition to its chromaticity.

3. Perceptual color spaces: these are color spaces based on perceptual parameters such as hue, purity, brilliance, brightness, and saturation. Many different perceptual color spaces will be defined, and a representative form is shown in fig (2.18).

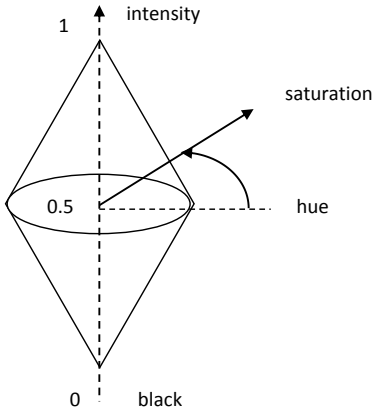

Figure (2.18) The form of the typical perceptual color [Nib1986]

2.11 Why is there more than one color space?

Different color spaces are better for different applications, for example some equipment has limiting factors that dictate the size and type of color space that can be used.

More common computer related color spaces. There many color spaces in the field of color representation, such color spaces are:-

1. **RGB** is a three dimensional color space whose components are the red, green, and blue intensities that makeup a given color. This is an additive color system based on tri-chromatic theory. Often found in systems that use a CRT (Cathode Ray Tube) to display images. RGB is easy to implement but non–linear with visual perception. It is device dependent and specification of colors is semi–intuitive. RGB is very common, being used in virtually every computer system as well as television, video etc. [App 1996**,** For 1998].
2. **YIQ** is used in NTSC (North America) television broadcasts for historical reason YIQ stores a luminance value with two chrominance values, corresponding approximately to the amounts of blue and red in the color. It corresponds closely to the YUV (also called YCC or more accurately YCbCr) scheme used in PAL television and JPEG image compression. Except for the fact that the YIQ color space is rotated 33^0 with respect to the YUV color space [Jab 2006].
3. **HSV** is often used by artists because it is often more natural to think

about a color in terms of hue and saturation than in terms of additive or subtractive color components. HSV stores a hue value a saturation value and intensity value [Jab 2006].

4. **HLS** this represents a wealth of similar color spaces, alternative names include HSI (intensity), HSV (value), HCI (chroma / colorfulness), HVC, TSD (hue saturation and darkness) etc. Most of these color spaces are linear transforms from RGB and are therefore device dependent and non–linear. Their advantage lies in the extremely intuitive manner of specifying color. It is very easy to select a desired hue and to then modify it slightly by adjustment of its saturation and intensity. The supposed separation of the luminance component from chrominance (color) information is stated to have advantages in applications such as image processing. However the exact conversion of RGB to hue, saturation and lightness information depends entirely on the equipment characteristics. Failure to understand this may account for the sheer numbers of related but different transforms of RGB to HLS, each claimed to be better for specific applications than the others.

5. **CIE** there are two CIE based color spaces, CIELuv and CIELab. They are nearly linear (as close as any color space is expected to sensibly get). CIELab and CIELuv are device independent but suffer from being quite unintuitive despite the L parameter having a good correlation with perceived lightness. CIEluv has an associated two-dimensional chromaticity chart which is useful for showing additive color mixtures, making CIELuv useful in applications using CRT displays. CIELab has no associated two dimensional chromaticity diagrams and no correlate of saturation [For 1998].

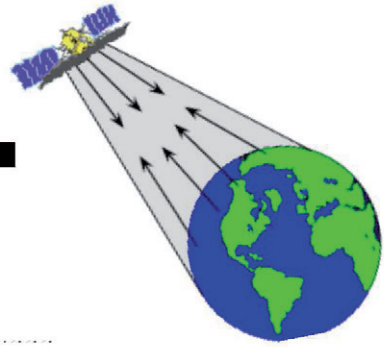

CHAPTER THREE

Image Fusion Methodologies

Image Fusion Methodologies

3.1 Introduction

Fusion is a set of methods and tools using data coming from various sources of different nature, in order to increase the quality of the requested information. Increasing information's quality implies that the signal after the fusion includes more helpful information than the original one. That, in turn, means that during the fusion process some new information is added into the original signal. In general, fusion aims at combining complementary information of a few sources. The scheme, representing the information distribution of two sources is depicted in fig. (3.1). Suppose that two sensors of different nature observe the same patch of land surface, the data coming from the first and the second sensor are denoted as S_1 and S_2, respectively.

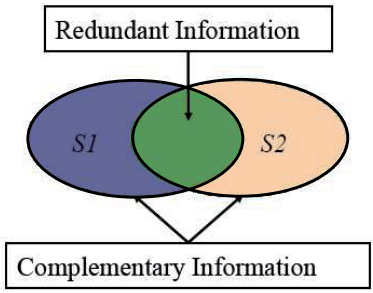

Figure (3.1): Information coming from two different sources [Bun 2004].

Since the sources exhibit dissimilarities (in abroad sense), the information can be divided into redundant (common for both sensors $S_1 \cap S_2$) and complementary (the information which is unique to either of the sensors –

$S_1 / (S_1 \cap S_2)$ and $S_2 / (S_1 \cap S_2)$). Therefore, the information difference of the datasets to be fused is a requirement for the fusion to be reasonable [Bun 2004]. In applications, we need more than one type of measurements to tell us everything we want to know about a process.

Data fusion can create scenes with better spatial and spectral resolution by merging two images of different spatial and spectral resolution. It is possible to have several images of the same scene providing different information, although the scene is the same. This is because each image has been captured with a different sensor. High spectral resolution allows identification of materials in the scene, while high spatial resolution locates those materials [Paj 2004, Gro 1998].

Every remotely sensed image has a specific limit of its own spectral and spatial resolution. There is no ideal sensor that is highly sensitive to all wavelengths and yields spatially detailed data. Though it is unfeasible to obtain a desired image, an image taken with a sensor can be complementarily used for images from other sensors. For example, recent satellite imaging systems including SPOT and Landsat Thematic Mapper (TM) simultaneously provide two complementary sets of image data, one of which has high spatial resolution and the other has low spatial resolution but is composed of several spectral bands. Moreover, a set of multispectral image data that has high spatial resolution can be used to enhance the resolution of another multispectral image data of lower resolution [Kan 2001].

In remote sensing, rapid developments of new satellites and more advanced sensor systems allow researches to have a wide spectrum of data for the same region of the Earth. The appropriate combination of information from these different sources might produce a product, which contains the information of higher quality and is more reliable for different applications in remote sensing. Such product, otherwise, might be difficult to obtain by other means or be totally unavailable because of different restrictions of the sensors, satellite's orbit, etc. Since the source data in remote sensing are images of the land surface, the combination process is called "*image fusion*". A sketch of image fusion is shown in fig. (3.2). As can be seen; the combination produced a scene with better enhanced features.

In this research, the problem of fusion images of different modulates is investigated, by utilizing different fusion's algorithms. High spatial resolution scenes are combined with enlarged blurred lower resolution "ETM+" images to produce several enhanced bands of "ETM+" images.

MS image

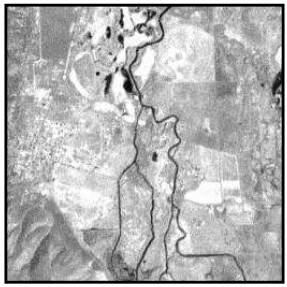

PAN image

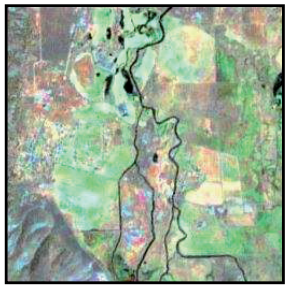

Unified image

Figure (3.2): Demonstration of image unification

3.2 Objectives of Image Fusion

Image fusion is a tool to combine multisource imagery using advanced image processing techniques. It aims to integrate the disparate and complementary data to enhance the information apparent in the images as well as to increase the reliability of the interpretation. This leads to more accurate data and increased utility. It is also stated that fused data provides more robust operational performance (i.e. increased confidence, reduced ambiguity, improved reliability and improved classification) [Poh 1998]. The related published work in the literature indicates that image fusion is applied to digital imagery in order to: [Poh 1998]

a. Sharpen images,
b. Improve geometric corrections,
c. Provide stereo-viewing capabilities for stereophotogrammetry,
d. Enhance certain features not visible in either of the single data alone,

e. Complement data sets for improved classification,
f. Detect changes using multitemporal data,
g. Substitute missing information (e.g., clouds-VIR, shadows-SAR) in one image with signals from another sensor image,
h. Replace defective data.

3.3 Fusion of Multispectral and Panchromatic Data

The main problem that may arise in the task of fusion of a multispectral with a panchromatic scene is the distortion in the chromatic information as the achromatic information changed. This can be happen because the chromatic information is not separated from the achromatic information (the brightness) when one fuses the images in the RGB color space. Therefore, most researchers use the perceptual color spaces to separate the chromatic information from the achromatic information, as a perceptual color space some researchers prefer the HSI color space without specifying which algorithm they used, while other researchers recommended the Lab color space without specifying why like Francisco [Roc 1998]. A comparison between the perceptual color spaces and their accuracy for image fusion has been performed in this research, on various tests, by conducting on a number of the most perceptual color spaces. The color spaces included in this study are classified into three kinds; i.e. HLS color space models, Lab color spaces models, and YUV color spaces models.

3.4 Conservation of the Mean Brightness of the Achromatic Information

One of the main artifacts in the field of fusing a multispectral image with the panchromatic one is the variation in the final produced brightness. This may happen when the replacement of the achromatic information is done by using panchromatic information that differs in the mean brightness from the achromatic information. The result will be either ultra-bright or too dark fused image when it is compared with the panchromatic image, even if the fused image contains very good spatial information [Jab 2006]. Adjusting the mean brightness of the panchromatic image with the achromatic part can be done by:

$$PAN_{New} = \frac{M_a}{M_{PAN}} \times PAN_{old} \quad \text{,..... (3.1)}$$

where

PAN is the panchromatic image, PAN_{New} is the adjusted panchromatic brightness that replaces the achromatic PAN_{old} information, M_a is the mean of the achromatic

information value, and M_{PAN} is the mean of the panchromatic information value [Jab 2006].

3.5 Principal Component Analysis (PCA) for Image Fusion

The PCA is mainly depends on *Hotelling or Karhunen-Loeve "KL"* transformation [Gon 2002]. Suppose *m* images want to be transformed, each of size $N \times N$ pixels. Each image *f(x, y)* can be expressed in the form of N^2-dimensional vector X_i, as follows:

$$X_i = \begin{bmatrix} x_{i1} \\ x_{i2} \\ . \\ x_{ij} \\ . \\ x_{iN^2} \end{bmatrix} \quad \text{,..... (3.2)}$$

Where: x_{ij} denotes the j^{th} component of vector X_i (representing i^{th} image), ascended as image row after row. For *m* tested images, an array of $N^2 \times m$ elements can be constructed, called space collection array; i.e.

$$A_{N^2,m} = \begin{bmatrix} a_{1,1} & a_{1,2} & ..... & a_{1,m} \\ a_{2,1} & a_{2,2} & ..... & a_{2,m} \\ . & . & ..... & . \\ a_{i,1} & a_{i,2} & ..... & a_{i,m} \\ . & . & ..... & . \\ a_{N^2,1} & a_{N^2,2} & ..... & a_{N^2,m} \end{bmatrix} \quad \text{,..... (3.3)}$$

The covariance matrix of *A is given by:*

$$Cov = E\{(A_{ij} - m_j).(A_{ij} - m_j)^T\} \quad \text{,..... (3.4)}$$

Where m_j is the mean of the j^{th} image within the space collection array, E {.} denotes the expectation operation, $(.)^T$ indicating matrix transposition and the mean reduced space collection array is given by:

$$(A_{ij} - m_j)^T = \begin{bmatrix} a_{1,1} & a_{2,1} & . & . & a_{N^2-1,1} & a_{N^2,1} \\ a_{1,2} & a_{2,2} & . & . & a_{N^2-1,2} & a_{N^2,2} \\ . & . & . & . & . & . \\ . & . & . & . & . & . \\ a_{1,m-1} & a_{2,m-1} & . & . & a_{N^2-1,m-1} & a_{N^2,m-1} \\ a_{1,m} & a_{2,m} & . & . & a_{N^2-1,m} & a_{N^2,m} \end{bmatrix} - \frac{1}{N^2} \begin{bmatrix} \sum_{i=1}^{N^2} a_{i,1} \\ \sum_{i=1}^{N^2} a_{i,2} \\ . \\ . \\ \sum_{i=1}^{N^2} a_{i,m-1} \\ \sum_{i=1}^{N^2} a_{i,m}. \end{bmatrix} \quad \text{,…….. (3.5)}$$

The *Cov* matrix is a symmetric array has m-Eigen vectors and Eigen-values. The array consisting the covariance Eigen vectors, as its rows, in ascending order represents the "KL" transformation kernel array; given by:

$$T=\begin{bmatrix} e_{1,1} & e_{2,1} & . & . & e_{N^2-1,1} & e_{N^2,1} \\ e_{1,2} & e_{2,2} & . & . & e_{N^2-1,2} & e_{N^2,2} \\ . & . & . & . & . & . \\ . & . & . & . & . & . \\ e_{1,m-1} & e_{2,m-1} & . & . & e_{N^2-1,m-1} & e_{N^2,m-1} \\ e_{1,m} & e_{2,m} & . & . & e_{N^2-1,m} & e_{N^2,m} \end{bmatrix} \begin{matrix} 1^{st} \text{ Eigen vector} \\ 2^{nd} \text{ Eigen vector} \\ . \\ . \\ (m-1) \text{ Eigen vector} \\ m^{th} \text{ Eigen vector} \end{matrix} \quad ,\ldots\ldots (3.6)$$

The KL-Transformation can be performed to compute the *j=1 to m* principal components as: $Y_j = T_{ij}(X_j - m_j) = \sum_{i=1}^{N^2} e_{ij}(x_{ji} - m_j)$,..... (3.7)

Let λj represents the jth Eigen value of the covariance matrix, corresponding to the jth Eigen vector Ej. It is well known that; the slighter order principal component carry higher informational energy than the upper order one, because λ1 ≥ λ2 ≥ · ≥ λm, due to the following diagonal matrix expressions, as illustrated in fig. (3.3);

$$D_{Diag} = T\,Cov\,T^T = \begin{bmatrix} \lambda_1 & & & 0 \\ & \lambda_2 & & \\ & & . & \\ 0 & & & \lambda_m \end{bmatrix} \quad ,..... (3.8)$$

Original colored scene

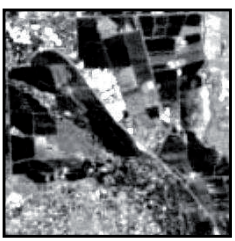

PCA-1

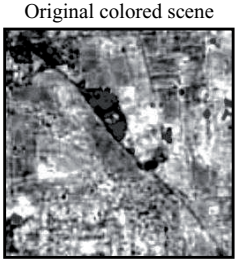

PCA-2

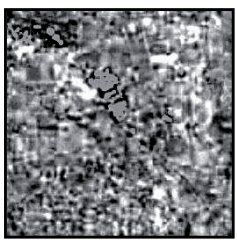

PCA-3

Figure (3.3): Illustration of color scene and its PCAs.

The principal Component Analysis fusion method can now perform by replacing the normalized brightness high resolution scene by the 1st *PCA* (i.e. PCA_1), and then inverse transform will be implemented as illustrated in the block diagram shown in fig. (3.4). Other *PCA* may be chosen to be replaced by the high resolution normalized brightness scene, but the result will not being encouraging.

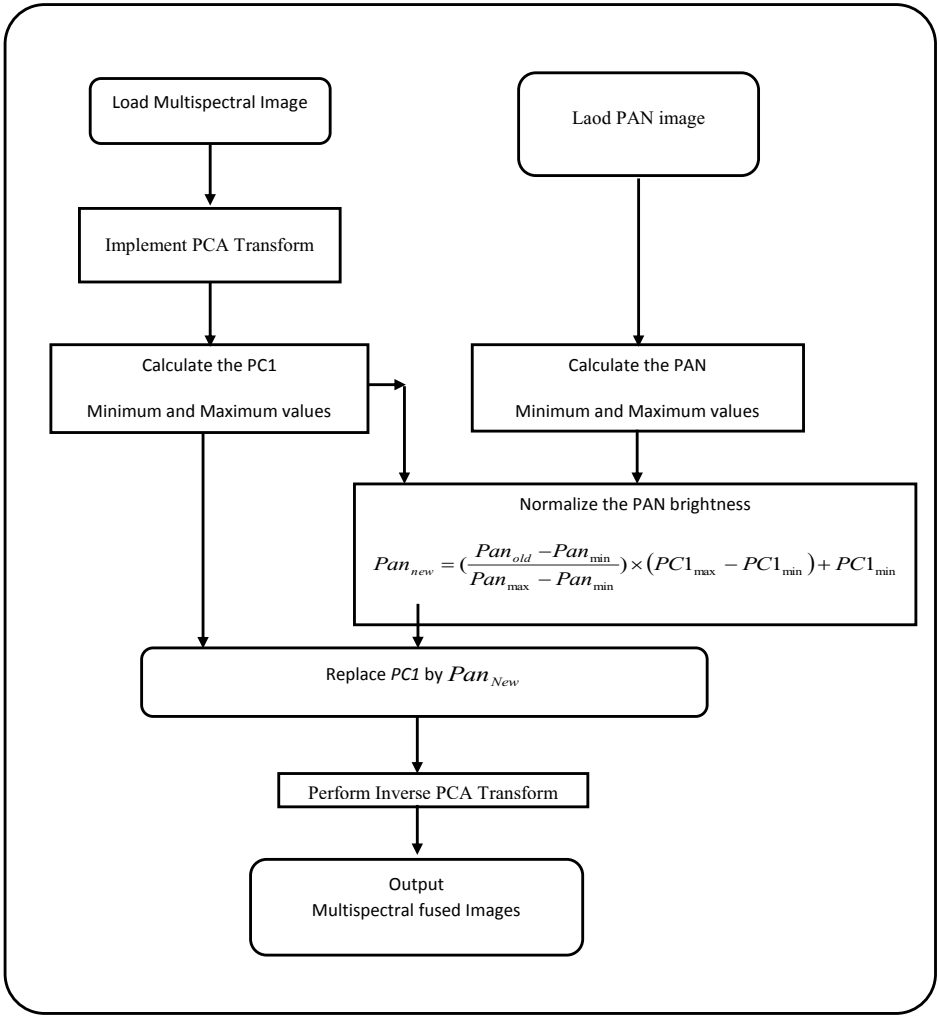

Figure (3.4): Block Diagram illustrating the procedures involved in the PAC fusion method.

3.6 The Wavelet Transform Fusion Formulation Methods:

Although the Fourier transform has been the basis of transform-based image processing since the late 1950s, a more recent transformation, called the *wavelet transform*, is now making it even easier to be implemented in different image processing applications. Unlike the Fourier transform, whose basis functions are sinusoidal, wavelet transforms are based on small waves, called *wavelets*, of varying frequency and limited duration. This allows them to provide the equivalent of a musical score for an image, revealing not only what notes (or frequencies) to play but also when to play them. Conventional Fourier transforms, on the other hand, provide only the notes or frequency information; temporal information is lost in the transformation process.

In 1987, wavelets were first shown to be the foundation of a powerful new approach to signal processing and analysis called multi-resolution theory [Mal 1987]. Multi-resolution theory incorporates and unifies techniques from a variety of orders, including sub-band coding from signal processing, quadrate mirror filtering from digital speech recognition, and pyramidal image processing. As its name implies, multi-resolution theory is concerned with the representation and analysis of signals (or images) at more than one resolution. The appeal of such an approach is obvious features that might go undetected at one resolution may be easy to spot at another. Although the imaging community's interest in multi-resolution analysis was limited until the late 1980s, it is now difficult to keep up with the number of papers, book, and books devoted to the subject, for instance see [Gon 2002].

Fig. (3.5) shows the principle of a two-band sub-band coding and decoding system.

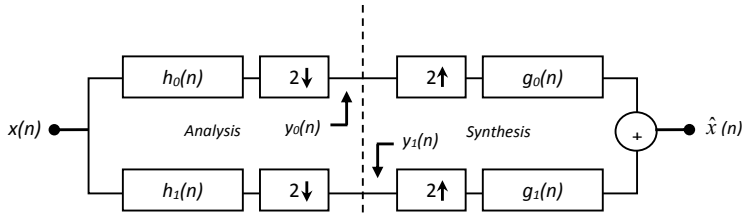

Figure (3.5): A two-band filter bank for one-dimensional sub-band coding and decoding.

A discrete-time signal x(n) for n = 0,1,2,..., the output sequence $\hat{x}(n)$ is formed through the decomposition of x(n) into y0(n)and y1(n) via analysis filters ho(n) and $h_1(n)$, and subsequent recombination via synthesis filters $g_0(n)$ and $g_1(n)$. A variety of wavelet transformations have been developed and implemented in wide range of

image processing. Among these, we shall chose two types which represent; the simplest one (*Haar wavelet*) and the most recent adaptive one named (*Tab3/5 wavelet transform)*.

3.6.1 The Haar Wavelet Transform:

The *Haar wavelet* is even simpler and most common used one. It is often used for educational purposes. It is separable, so it can be used to implement a wavelet transform by first convolving it with the rows and then with the columns [Umb 1998]. The Haar basis vectors are simply:

$$\text{LOWPASS: } \frac{1}{\sqrt{2}}\begin{bmatrix} 1 & 1 \end{bmatrix} \quad \text{,..... (3.9)}$$

$$\text{HIGHPASS: } \frac{1}{\sqrt{2}}\begin{bmatrix} 1 & -1 \end{bmatrix} \quad \text{,..... (3.10)}$$

The wavelet transform is performed as follows [Umb 1998]:

1. Convolve the low pass filter with the image rows (by sliding, multiplying coincident terms, and summing the results),
2. Convolve the low pass filter with the columns (of the results from step 1) and sub sample this result by taking every other value; this gives us the low pass-low pass version of the image,
3. Convolve the result from step 1, the low pass filtered rows, with the high pass filter on the columns. Sub sample by taking every other value to produce the low pass-high pass image,
4. Convolve the original image with the high pass filter on the rows and save the result,
5. Convolve the result from step 4 with the low pass filter on the columns; sub sample to yield the high pass-low pass version of the image,
6. To obtain the high pass-high pass version, convolve the columns of the result from step 4 with the high pass filter.

Fig. (3.6) represent examples of different levels of ***Haar transformation.***

(a)Input image

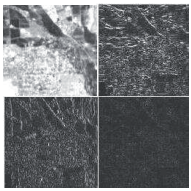

(b) 1st level Transformed image

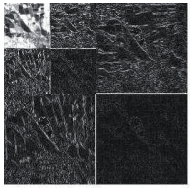

(c)2nd level Transformed Image

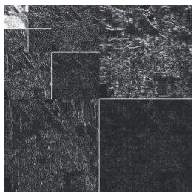

(d) 3rd level Transformed image

Figure (3.6): Examples of a discrete wavelet transform using Haar basis functions. (b)- (d) Several different levels of transformations.

The inverse wavelet transform is performed by size's doubling (Up sampling) the sub-bands to its original size; i.e. insert zeros between each of the four sub images, and sum the results to obtain the original image. For the Haar filter, the inverse wavelet basis vectors are identical to the forward filters.

3.6.2 Bi-Orthogonal Tab3/5 filters

In this transformation, the sequence of simple filtering operations for which alternately, odd pixel values are updated with a weighted sum of odd pixel values and is rounded to an integer value, and even pixel values are updated with a weighted sum of odd pixel values and also rounded to an integer value. The odd coefficients of the output pixel C are computed first for all values of x such that $-1 \leq 2x+1 \leq W+1$:

$$C(2x+1) = C_{ext}(2x+1) - \frac{C_{ext}(2x) + C_{ext}(2x+2)}{2} \quad , \ldots\ldots\ldots\ldots\ldots (3.11)$$

Where; W is the original image width.

Then the even coefficients of the output signal C can now computed from the even values of extended pixel Cext, and the odd coefficients of pixel C for all values of x such that $-1 \leq 2x+1 \leq W+1$ [Moh 2006]:

$$C(2x) = C_{ext}(2x) + \frac{C_{ext}(2x-1) + C(2x+1) + 2}{4} \quad , \ldots\ldots\ldots\ldots\ldots (3.12)$$

This procedure is applied in both directions (vertical and horizontal) to get the final transformed image [Moh 2006]. Examples of several levels of discreet ***Tab3/5 wavelet*** transformations are illustrated in fig. (3.7).

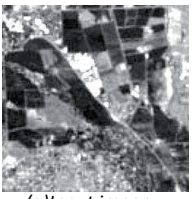

(a)Input image

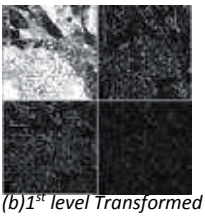

(b)1st level Transformed

(c)2nd level Transformed

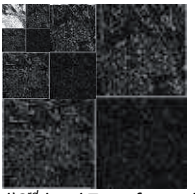

(d)3rd level Transformed image

Figure (3.7): Examples of a discrete wavelet transform using* Tab3/5 *basis functions. (b)- (d) Several different levels of transformations.

3.7 Wavelet Fusion Methods:

In order to perform the WT fusion, images should be decomposed to a desired level; in this project the 1st, 2nd and 3rd level are adopted, as it has been found yielding best fusion result. The fusion processes involved in this method are illustrated in the block-diagram shown in fig. (3.8). For each level, 4 sub-bands, contain the color information, are created. The low-low band of the last level from ETM+ image is replaced by the same sub-band of the PAN image. An inverse WT should then be applied to produce the unified ETM+ scene [Ven 2002]. The procedures mentioned above should be repeated with each band of the multispectral ETM+ scene.

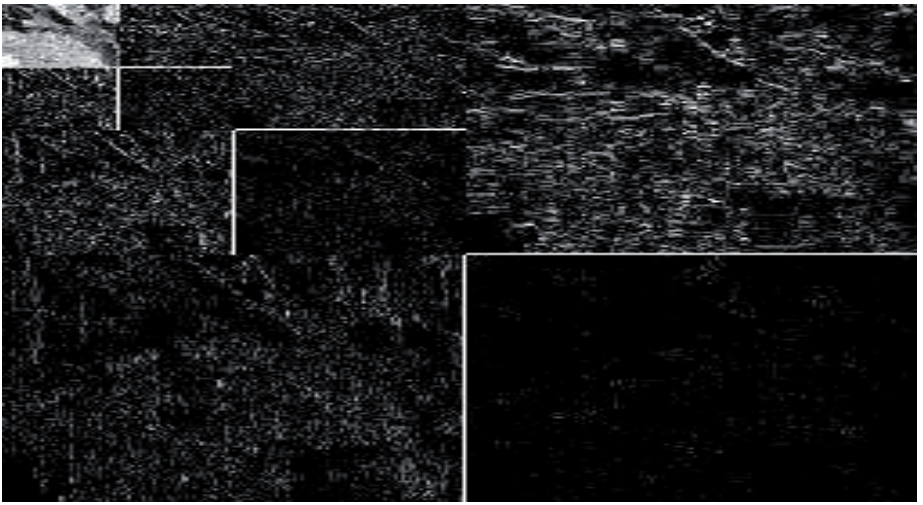

3.8 Color Space Transformation Formula

The use of color in image processing is motivated by two principal factors; it is a powerful descriptor that often simplifies object identification, also humans can discern thousands of color shades and intensities, compared to about only two dozen shades of gray. Color image processing is divided into two major areas: full-color and pseudocolor processing. In the first category, images are acquired with a full-color sensor, such as a color TV camera or color scanner. In the second category, the problem is one of assigning a color to a particular monochrome intensity or range of intensities. Until recently, most digital color image processing was done at the pseudocolor level [Gon 2002].

In color spaces literatures there are many color spaces defined as perceptual color spaces, and some perceptual color spaces can be computed by more than one algorithm. In this research, several perceptual colors will be tested, using different transformations. The Lab, YUV and HLS color spaces are the most well known of them, thus are adopted to perform image fusion.

3.8.1 The CIE-RGB Color Space:

The CIE (*Commission International de l'Eclairage* /or International Commission on Illumination) chromaticity diagram, fig.(3.9), shows color composition as a function of x (red) and y (green), while the corresponding value of z (blue), z = 1 -(x + y).

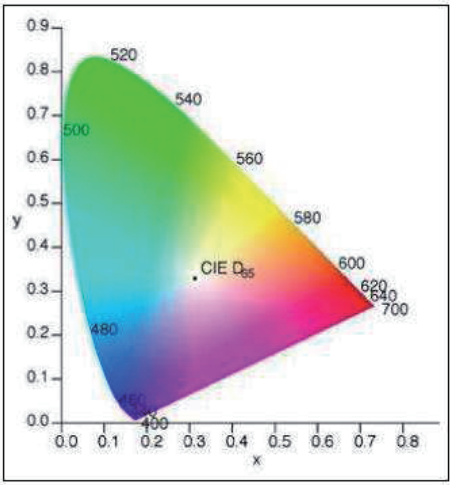

Figure (3.9): C.I.E. Chromaticity Diagram [Gon 2002].

The point marked green has approximately 62% green and 25% red content, while the composition of blue is approximately 13%. The positions of the various spectrum colors—from violet at 380 nm to red at 780 nm—are indicated around the boundary of the tongue-shaped chromaticity diagram. Any point not actually on the boundary but within the diagram represents some mixture of spectrum colors. The point referred ***equal energy*** corresponds to equal fractions of the three primary colors; it represents the CIE standard for white light. The chromaticity diagram is useful for color mixing because a straight-line segment joining any two points in the diagram defines all the different color variations that can be obtained by combining these two colors additively [Gon 2002].

The color representation system has great importance in many color processes, and in particular in computer graphics. All the color representation systems imply reduction of the spectral color space to a finite-dimensional space. For the purposes of color perception, the human eye works as a three dimensional receptor, with sensors that sample the spectrum at the red, green, and blue regions of the visible spectrum.

$$\lambda_1 = 700 \quad nm\ (red),\ \lambda_2 = 546 \quad nm\ (green),\ \lambda_3 = 435.3\ nm\ (blue)$$

As a standard, the CIE-RGB model has several drawbacks [Jab 2006]:

A. The primary basis does not span the whole color solid.
B. The color reconstruction functions take negative values, which complicate the calculation of a color's coordinates starting from its spectral distribution. One must compute the negative part separately, and then subtract.

C. In order to obtain the achromatic point with chromaticity coordinates (1/3, 1/3, 1/3), it is necessary to change the scales of the primary colors; so that the region under the graph of each color reconstruction function does not have the same area.

3.8.2 The CIE-XYZ Standard

Due to the problems in the CIE-RGB space, the CIE established (in 1931) a new standard, with primary colors X, Y, and Z, that is designed to simplify, as much as possible, calculations involving colorimetric magnitudes. For this purpose, the primaries satisfy the following conditions [Jab 2006]:

A. All XYZ components for all visible colors are nonnegative.
B. Two of the primaries have zero luminance.
C. There are many spectral colors that have at least one zero XYZ component.

Not all colors in the CIE-XYZ system are physically realizable. We can obtain the colorimetric magnitudes of color in this system in terms of those in the CIE-RGB system, see fig. (3.10). It can be considered as to be an improved version of the CIE-RGB color system, thus it is usually used in the color systems conversion as intermediate color space (such as from RGB to Lab), will be discussed in the next section.

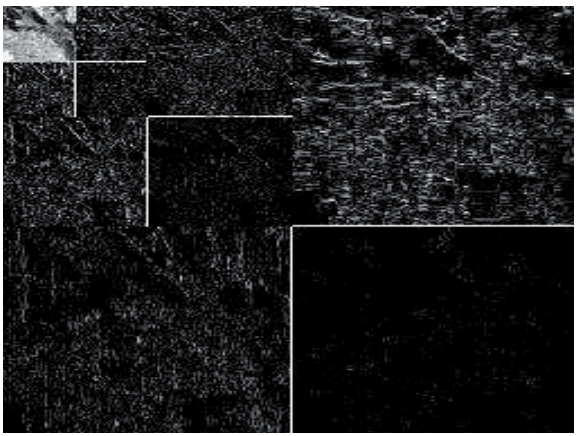

Figure (3.10): The color cube sits within the CIE XYZ system **[Log 2005].**

The Logicol algorithms for the XYZ spaces have been tested and found suitable to be used in the fusion algorithms, the steps are given in the CIE-Lab model bellow [Log 2005].

3.8.3 The CIE-Lab Uniform Color Model

A ***Lab* color space** is a color-opponent space with dimension ***L*** for lightness and ***a*** and ***b*** for the color-opponent dimensions, based on nonlinearly-compressed CIE XYZ color space coordinates.

Where the CIE-Lab uniform color space was introduced by the CIE group, but it is recommended for modeling the reflected light condition. The color transformation formula is given by the following transformation procedures [Log 2005]:

RGB → XYZ Transformation Steps

$$R' = \begin{cases} \left(\dfrac{\dfrac{R}{255} + 0.055}{1.055} \right)^{2.4} \times 100 & if \ \dfrac{R}{255} > 0.0405 \\ \dfrac{\dfrac{R}{255}}{12.92} \times 100 & otherwise \end{cases}$$

$$G' = \begin{cases} \left(\dfrac{\dfrac{G}{255} + 0.055}{1.055} \right)^{2.4} \times 100 & if \ \dfrac{G}{255} > 0.0405 \\ \dfrac{\dfrac{G}{255}}{12.92} \times 100 & otherwise \end{cases}$$

$$B' = \begin{cases} \left(\dfrac{\dfrac{B}{255} + 0.055}{1.055} \right)^{2.4} \times 100 & if \ \dfrac{B}{255} > 0.0405 \\ \dfrac{\dfrac{B}{255}}{12.92} \times 100 & otherwise \end{cases}$$

, $Y = 0.2126R' + 0.7152G' + 0.0722B'$ $X = 0.4124R' + 0.3576G' + 0.1805B'$

$Z = 0.0193R' + 0.1192G' + 0.9505B'$

XYZ → Lab Transformation Steps

$$L = 10\sqrt{Y}$$

$$a = 17.5\left(\frac{1.02X - Y}{\sqrt{Y}}\right)$$

$$b = 7\left(\frac{Y - 0.847Z}{\sqrt{Y}}\right)$$

The inverse transformation as given below is, also, performed by two operational steps:

1. First steps are used to convert the Lab bands into XYZ bands;

Lab → XYZ Transformation

$$Y' = \frac{L + 16}{116}$$

$$X' = \frac{a}{500} + Y'$$

$$Z' = Y' - \frac{b}{200}$$

$$X' = \begin{cases} X'^3 & if\ X'^3 > 0.008856 \\ \dfrac{X' - \dfrac{16}{116}}{7.787} & otherwise \end{cases}$$

$$Y' = \begin{cases} Y'^3 & if\ Y'^3 > 0.008856 \\ \dfrac{Y' - \dfrac{16}{116}}{7.787} & otherwise \end{cases}$$

$$Z' = \begin{cases} Z'^3 & if\ Z'^3 > 0.008856 \\ \dfrac{Z' - \dfrac{16}{116}}{7.787} & otherwise \end{cases}$$

$$X_{ref} = 95.047$$

$$Y_{ref} = 100.000$$

$$Z_{ref} = 108.883$$

$$X = X_{ref} X'$$

$$Y = Y_{ref} Y'$$

$$Z = Z_{ref} Z'$$

2. Converting the XYZ bands back to the original RGB bands;

XYZ → RGB

$$, \; Z' = \frac{Z}{100}, \; Y' = \frac{Y}{100} \; X' = \frac{X}{100}$$

$$, \; G' = -0.9689X' + 1.1.8758Y' + 0.0415Z' \; R' = 3.2406X' - 1.5372Y' - 0.0415Z'$$
$$B' = 0.0557X' - 0.2040Y' + 1.0570Z'$$

$$R = \begin{cases} (1.055R'^{\frac{1}{2.4}} - 0.055) \times 255 & if \; R' > 0.0031308 \\ 12.92R' \times 255 & otherwise \end{cases}$$

$$G = \begin{cases} (1.055G'^{\frac{1}{2.4}} - 0.055) \times 255 & if \; G' > 0.0031308 \\ 12.92G' \times 255 & otherwise \end{cases}$$

$$B = \begin{cases} (1.055B'^{\frac{1}{2.4}} - 0.055) \times 255 & if \; B' > 0.0031308 \\ 12.92B' \times 255 & otherwise \end{cases}$$

While CIE-Lab is claimed to provide an accurate representation of color, as perceived by humans, it does not provide a very intuitive one. It is not trivial to find common color locations as it is not immediately clear what the axes actually represent. A careful observation of these uniform spaces shows that they are organized after opponent-processes models: L is the lightness (achromatic) axis, while a (R-G) and b (Y-B) are the chromatic opponent-processes axes, where positive a values represent red, negative ones represent green, positive b values represent yellow, and negative ones represent blue. But this is not immediately obvious, and has never been explicitly mentioned in these spaces specifications. Even after observing the opponent-processes nature CIE-Lab, it is still useful to obtain a relationship between this space coordinate and most common perceptual axes (lightness, hue, and saturation) [Jab 2006] fig (3.11) shown L,a and b spaces.

(a)

(b)

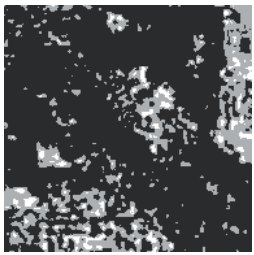

(c)

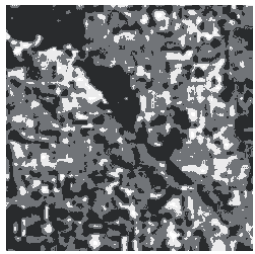

(d)

Figure (3.11): Lab transformation (a). Original image, (b). L band, (c). a - band, (d). b - band.

3.8.4 YUV Color Space

The YUV color space model defines in terms of one luma and two chrominance components. The YUV color model is used in the PAL, NTSC, and SECAM composite color video standards. Previous black-and-white systems used only luma (Y) information and color information (U and V) was added so that a black-and-white receiver would still be able to display a color picture as a normal black and white pictures. YUV models human perception of color in a different way than the standard RGB model used in computer graphics hardware. Y stands for the luma component (the brightness); U and V are the chrominance (color) components [Wik 2005] fig. (3.12) show Y, U and V spaces. The YUV space model that mentioned by Bourgin [Bou 1994] was tested in this research work and found reliable to be used in the fusion algorithms, the matrices of this model are:

RGB → YUV Transformation

$$\begin{bmatrix} Y \\ U \\ V \end{bmatrix} = \begin{bmatrix} 0.299 & 0.587 & 0.114 \\ -0.147 & -0.289 & 0.436 \\ 0.615 & -0.515 & -0.100 \end{bmatrix} \begin{bmatrix} R \\ G \\ B \end{bmatrix}$$

YUV→RGB Transformation

$$\begin{bmatrix} R \\ G \\ B \end{bmatrix} = \begin{bmatrix} 1 & 0.000 & 1.140 \\ 1 & -0.396 & -0.581 \\ 1 & 2.029 & 0.000 \end{bmatrix} \begin{bmatrix} Y \\ U \\ V \end{bmatrix}$$

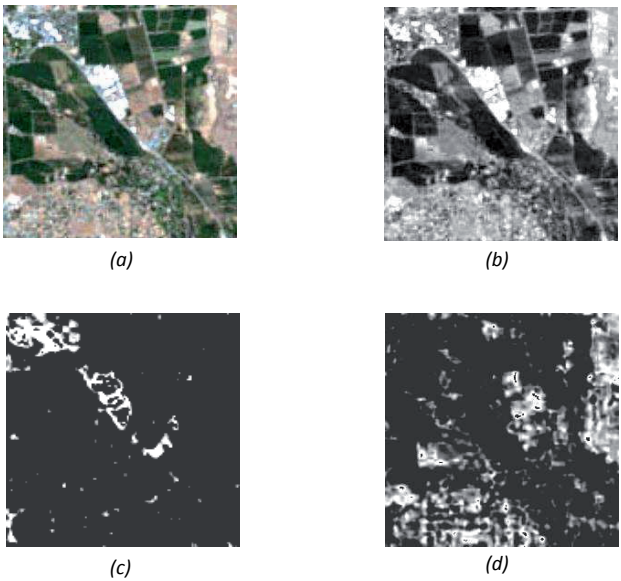

Figure (3.12): YUV transformation (a). Original image, (b).Y band, (c).U band, (d).V band.

3.8.5 HLS Color Space (HLS -Hexagonal)

1. There are two algorithms for HLS -Hexagonal space, one of them is the HIS-Hexagonal space model (used in display devices) that mentioned by Liao [Lia 1999]. And the second algorithm is:
2. The HLS-Hexagonal space algorithm that mentioned by Logicol S.r.l [Log 2005], was tested and found reliable to be used in the fusion systems, fig. (3.13) shown H, L, and S spaces ,the involved equations of this model are:

RGB → HLS Transformation

$$R_n = \frac{R}{255},\ G_n = \frac{G}{255},\ B_n = \frac{B}{255}$$

M = max(R_n,G_n,B_n)

m = min(R_n,G_n, B_n)

Δ = Max - Min

$$L = \frac{M+m}{2}$$

if Δ = 0 then

H = 0

S = 0

else

$$S = \begin{cases} \dfrac{\Delta}{M+m} & if\ L < 0.5 \\ \dfrac{\Delta}{2-M-m} & otherwise \end{cases}$$

$$R' = \frac{\frac{M-R_n}{6} + \frac{\Delta}{2}}{\Delta}$$

$$G' = \frac{\frac{M-G_n}{6} + \frac{\Delta}{2}}{\Delta}$$

$$B' = \frac{\frac{M-B_n}{6} + \frac{\Delta}{2}}{\Delta}$$

$$H = \begin{cases} B'-G' & if\ R_n = M \\ \frac{1}{3} + R'-B' & if\ G_n = M \\ \frac{2}{3} + G'-R' & if\ B_n = M \end{cases}$$

$$H = \begin{cases} H+1 & if\ H < 0 \\ H-1 & if\ H > 1 \end{cases}$$

endif

HLS → RGB Transformation

If S = 0

R =L * 255

G = L * 255

B = L* 255

else

$$i2 = \begin{cases} L(1+S) & if\ L < 0.5 \\ (L+S) - SL & otherwise \end{cases}$$

$i1$ = 2L - $i2$

R = 255 Hue_2_RGB($i1$, $i2$, H + $\frac{1}{3}$)

G = 255 Hue_2_RGB($i1$, $i2$, H)

B = 255 Hue_2_RGB($i1$, $i2$, H - $\frac{1}{3}$)

endif

Where Hue_2_RGB(v1, v2, H) is a function defined as:

if (H < 0) then H = H+1

elseif (H > 1) then H = H-1

$$Hue\_2RGB = \begin{cases} v1 + 6H(v2 - v1)\ if\ H < \frac{1}{6} \\ v2 \quad if\ \frac{1}{6} \le H < \frac{1}{2} \\ v1 + 6(v2 - v1)(\frac{2}{3} - H)\ if\ \frac{1}{2} \le H < \frac{2}{3} \\ v1 \quad if\ \ H > \frac{2}{3} \end{cases}$$

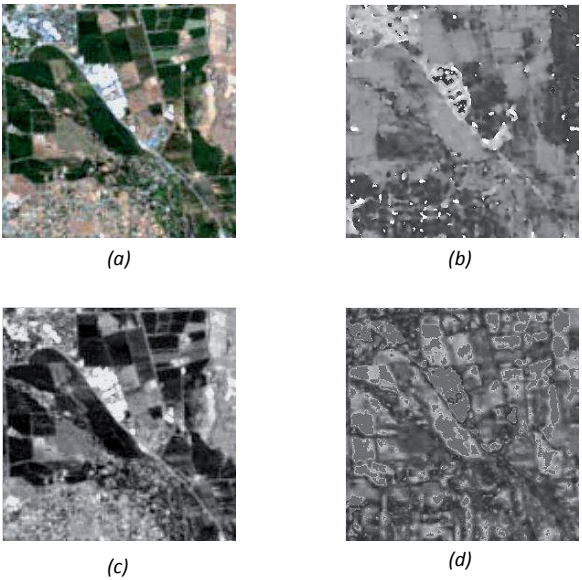

(a) *(b)*

(c) *(d)*

Figure (3.13): HLS transformation (a). Original image, (b).H band, (c).L band, (d).S band.

3.9 Color Space-based fusion

Image fusion based on color transformation is one of the oldest methods for sharpening of multisensor data.

In our fusion research we based on three color transformation (HLS, Lab, and YUV).

HLS (Hue- Lightness-Saturation) space fusion can be employed to sharpen the multispectral image by replacing L-band (comes from preceding image) by panchromatic image (PAN).

Firstly, three components of the original image *R*, *G* and *B* are transformed into the HLS color space. The transformation is given by the HLS procedure above.

After the transformation, the low-resolution Intensity component L is replaced by the panchromatic band with higher spatial resolution,

The final step is to transform the image back to *RGB* color space with the original values of *H* and *S*.

Lab space fusion done by the following steps:

- First we convert only Multispectral image(excluding PAN image from converting) from RGB to XYZ space by using the formula was shown above and then

- Converting from XYZ to Lab space,
- In Lab space we replace L-band by PAN image then,
- Reversing the transformation upward RGB enhanced image.

YUV space fusion done by converting just multispectral image from RGB to YUV space then replace Y-band by PAN image, then backward the transformation to yield fused image.

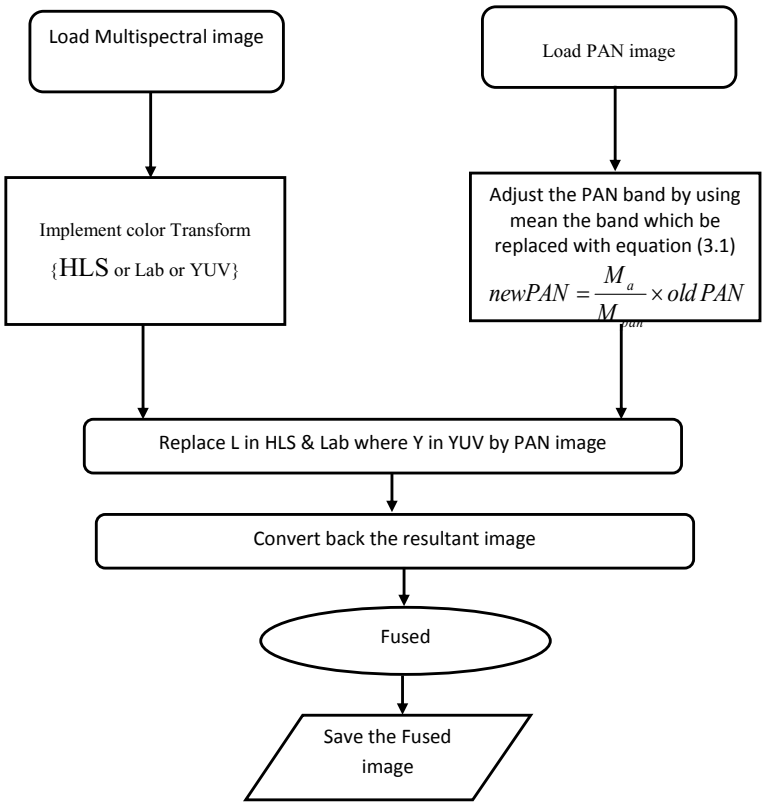

Figure (3.14) diagram shown image fusion by color transforms

3.10 Image Quality Criterion

With the development of new digital techniques for image coding and image processing, the need for reliable methods to measure image quality has increased accordingly. Evaluation of image quality is not only necessary to select the best

algorithms among a set of possible candidates, but also to optimize parameter settings.

There are many ways for measuring the fidelity "quality" of picture. These methods were classified in two categories:

(1) Objective assessment of image quality.

(2) Subjective assessment of image quality.

3.10.1 Objective Assessment of Image Quality:

The processing techniques that deal with digital images like enhancement, restoration, interpolation, etc may produce some errors in the reconstructed images. So that, objective fidelity criterion is one of the proceeding ways to find the acceptable level of quality of the output image "g*(x,y)"* that must be as close as possible to the original one "*f(x,y)"*.

A very commonly measure of image quality may give in the forms [had 2001]:

1) $MSE = \frac{1}{M \times N} \sum_{x=1}^{M} \sum_{y=1}^{N} (f(x,y) - g(x,y))^2$

2) $NMSE = \frac{MSE}{(M \times N)^{-1} \sum_{x=1}^{M} \sum_{y=1}^{N} f(x,y)^2}$

3) $RMSE = \sqrt{(MSE)}$, …… (3.13)

4) *Signal To Noise Ratio* $SNR(dB) = 10 \log_{10} \left(\frac{Power}{MSE} \right)$

5) *Peak – Signal To Noise Ratio* $PSNR = 10 \log_{10} \left(\frac{255^2}{MSE} \right)$

Where MxN represents image size.

The ***first, fourth*** *and* ***fifth*** methods will be used in our research. It is important to say, that until this day, it has proved practically impossible to formulate objective criteria for image quality, because of uncompleted reliability on heuristic approaches that objective quality rely on. For instance, computer remains unable to distinguish between "sharp" and "blurred" images. Therefore, removal of image blur is often an interactive process in which the user constantly has decide whether a result is acceptable [Had 2001].

1. Mean Square Error (MSE)

The first criterion is *Mean Square Error,* which is important to assess the overall difference may exist between the original image and its reconstructed version (i.e., the error/difference image energy). MSE could be determined by using the following equation [Gon 1987]:

$$MSE = \frac{1}{N \times M} \sum_{y=0}^{N-1} \sum_{x=0}^{M-1} [f(x,y) - g(x,y)]^2 \qquad \text{,..... (3.14)}$$

Where, g(x,y) denotes the reconstructed image pixel value at the locations x, and y.

2. Signal-to-Noise Ratio (SNR)

The most commonly used objective measures to compare two images are the root-mean-square error RMSE [Umb 1998]. The comparison between the images by using RMSE is differential, for this reason another criterion (derived from the root-mean-square error) with no units to make more objective comparison. This unit-less criterion is called signal-to noise ratio:

If f(x,y) is original image and g(x,y) is the restored one, then the mean square error MSE can be calculated by [Sta 1998]

$$MSE = \frac{1}{N \times M} \sum_{y=0}^{N-1} \sum_{x=0}^{M-1} [f(x,y) - g(x,y)]^2 \qquad \text{,..... (3.15)}$$

The signal-to-noise ratio (SNR) corresponding to the above error is

$$SNR_{db} = 10 \log_{10} \left(\frac{1}{MSE} \right) \qquad \text{,..... (3.16)}$$

And it is expressed in terms of decibels (dB); these objective measurements are often used in research because they are easy to generate and seemingly unbiased [Umb 1998].

3. Peak-Signal to Noise Ratio (PSNR)

Many signals have a very wide dynamic range; PSNR is usually expressed in terms of the logarithmic decibel scale. The phrase peak signal-to-noise ratio, often abbreviated PSNR, is an engineering term for the ratio between the maximum value of a signal and the magnitude of background noise. Because the PSNR is most commonly used as a measure of quality, it is determined for the 8-bit per pixel image band according to the following equation [Moh 2006]:

$$PSNR = 10\ Log_{10}\left[\frac{255^2}{MSE}\right] \qquad \text{,……..…… (3.17)}$$

3.10.2 Subjective Assessment of Image Quality:

This type of measurement is usually used when the output images are to be viewed by people as in the case of TV images. It is interested in how good the images look to human observers. The human visual system (HVS) has special characteristics, so those two pictures having the same amount of an objective criterion (MSE) may appear to have very different visual qualities [Had 2001].

Perceived image quality is assessed by different ways for example:

1) A quality scaling experiment, subjects are asked to classify images into a number of categories. For example: bad, poor, fair, good, and excellent. In a similar way, descriptive impairment and comparison scales have been defined.

2) The observers can make a comparison between the original and the processed one at a one displaying time then give the result.

CHAPTER FOUR

Experimental Results

Experimental Results

4.1 Introduction

In this chapter, the unification results obtained by the fusion algorithms discussed in chapter three, will be demonstrated and compared. Qualitative test might be carried by viewing the obtained results, and a quantitative test will be given numerically in terms of the Mean-Square-Error "MSE", Signal-to-Noise ratios "SNR", and Peak-Signal-to-Noise ratios "PSNR", between the original high-resolution PAN images, and the improved fused images. Samples of test images, representing Mousel-City, North Iraq (Original natural colored ETM_+ which will be fused with the monochromatic Spot-Panchromatic "PAN"), are shown in fig. (4.1). The fusion results will be investigated and discussed, depending on the implanted unifying methods; i.e.

1) Wavelet Transformation;
2) Color Transformation; and
3) Principle Component Analysis Transformation.

4.2 The Wavelet Fusion Techniques:

Two types of wavelet transformations have been adopted and used to fuse the samples of images, illustrated in fig. (4.1); these are ***Haar*** and ***Tap3/5*** wavelet transformation algorithms. Image resizing has been performed differently by;

1) *Nearest Neighbor;*
2) *Bilinear Interpolation; and*
3) *Cubic Convolution Interpolation.*

As mentioned under each image's samples; i.e. the ETM+ scene has been expanded 2.85 times to have same size as the PAN image.

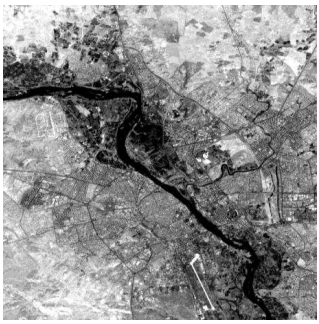

(a) PAN (Spot-Panchromatic, 10m resolution) image.

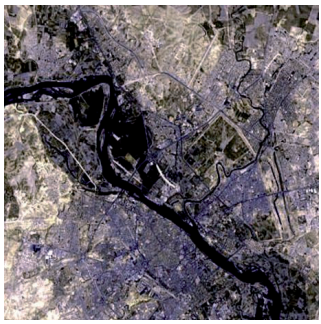

(b) ETM+ [(natural colored, bands 1,2,and 3), 28.5m resolution]image.

(c) Extracted Region from (a).

(d) Extracted region from (b) and expanded 2.85 times, using Bilinear method.

Figure (4.1): Samples of Mousel-City images; (a) Spot-Panchromatic "PAN", (b) Original natural colored ETM_+, (c) Extracted 256×256 pixels from PAN,(d) Extracted 256×256 from ETM_+.

4.2.1 The Haar Wavelet Transform Fusion Technique:

This fusion technique has been implemented in different ways (using different transformation levels), as illustrated in figs. (4.3 $\rightarrow$ 4.5); i.e.

1. Replacing the 1st level Low-Low quarter of the ETM+ image by the same transform level Low-Low of the PAN image.
2. Replacing the 2nd level Low-Low sub-quarter of the ETM+ image by the same transform level Low-Low of the PAN image.
3. Replacing the 3rd level Low-Low sub-quarter of the ETM+ image by the same transform level Low-Low of the PAN image.

4. Figure (4.2) illustrates the interface menu of the Visual basic program Ver.6 that has been designed to perform the DWT fusion technique.

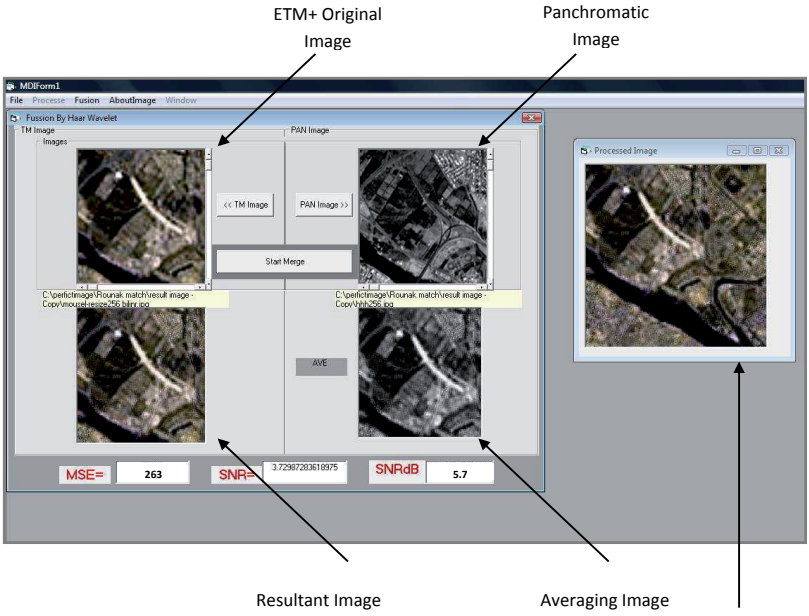

Figure (4.2): Program Interface menu for Haar Wavelet Fusion

(a) ETM+ resized by nearest neighbor method.

(b) Fused image by Haar 1st level WT.

(c) ETM+ resized by bilinear method.

(d) Fused image by Haar 1st level WT.

(e) ETM+ resized by Cubic Convolution.

(f) Fused image by Haar 1st level WT.

Figure (4.3): left side representing low resolution ETM+ images resized differently, while the right side representing their fused versions.

(a)

(b)

(c)

(d)

(e)

(f)

Figure (4.4): Same as in fig. (4.2,) but using 2nd level DWT method.

(a)

(b)

(c)

(d)

(e)

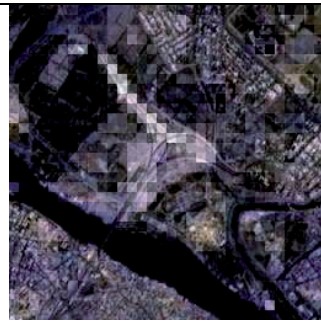

(f)

Figure (4.5): Same as in figs. (4.2 and 4.3), but using 3rd level DWT method.

4.2.2 The Tap 3/5 Wavelet Transform Fusion Technique:

This fusion technique has been performed by the same way, but replacing the Haar by the Tap 3/5 transformation. Fig (4.6) shows the interface menu of the designed Visual basic program, while the results are demonstrated in figs. (4.7 → 4.9).

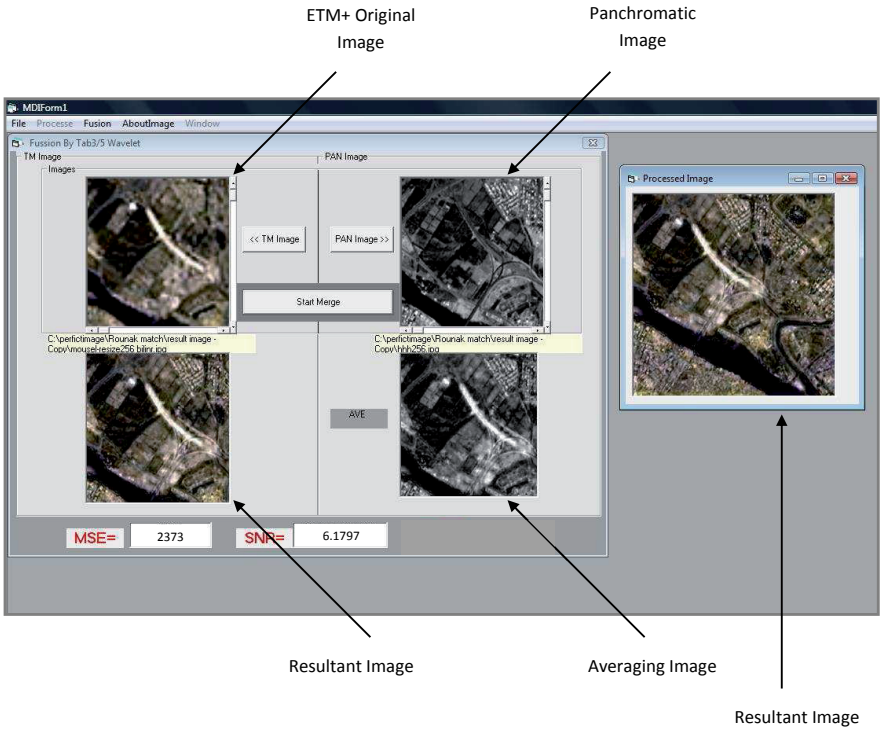

Figure (4.6): Program Interface menu of the DWT Tab3/5 Fusion Method.

(a)

(b)

(c)

(d)

(e)

(f)

Figure (4.7): Same as fig. (4.2), but using Tap 3/5 DWT.

(a)

(b)

(c)

(d)

(e)

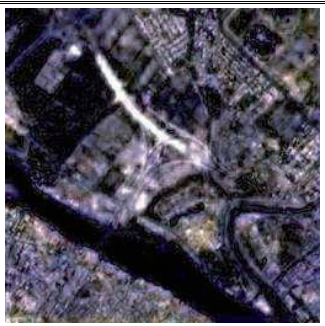

(f)

Figure (4.8): Same as fig. (4.3), but using Tap 3/5 DWT.

(a)

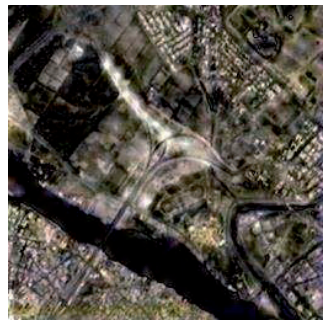

(b)

(c)

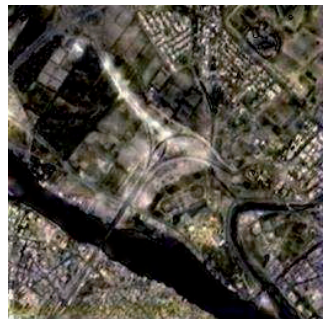

(d)

(e)

(f)

Figure (4.9): Same as fig. (4.4), but using Tap 3/5 DWT.

4.3 Color Transformation Fusion Techniques

Different color transformation (i.e. HLS, Lab, and YUV) techniques have been adopted and used to unifying samples of different resolution images; This fusion technique has been implemented in different ways, as illustrated in figs.(4.13 $\rightarrow$ 4.15) respectively; i.e.

HLS(Hue-Lightness-Saturation) space fusion can be implemented by replacing L-band (comes from multispectral image) by panchromatic image (PAN); it's done by:

1. Three components of the original image *R*, *G* and *B* are transformed into the HLS color space.
2. Then the low-resolution Intensity component L is replaced by the panchromatic band with higher spatial resolution.
3. The final step is to transform the image back to *RGB* color space with the original values of *H* and *S*.
4. Visual basic program Version 6 has been used to test HLS fusion results, fig. (4.10) illustrate the interfacing program.

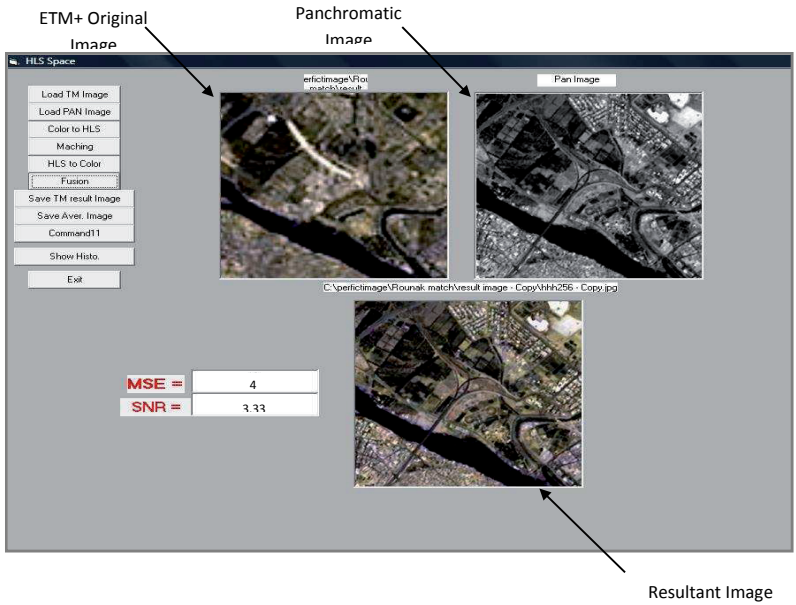

Figure (4.10): Program Interface menu for HLS Fusion Method.

Lab space fusion done by the following steps:

1. Convert Multispectral image from RGB to XYZ space using the formula described in chapter three, section 3.8.3,
2. Converting from XYZ to Lab space,
3. Replace L-band by PAN image then,
4. Reversing the transformation upward RGB enhanced image.
5. Visual basic program Version 6 has been used to test Lab fusion results, fig. (4.11) illustrate the interfacing program.

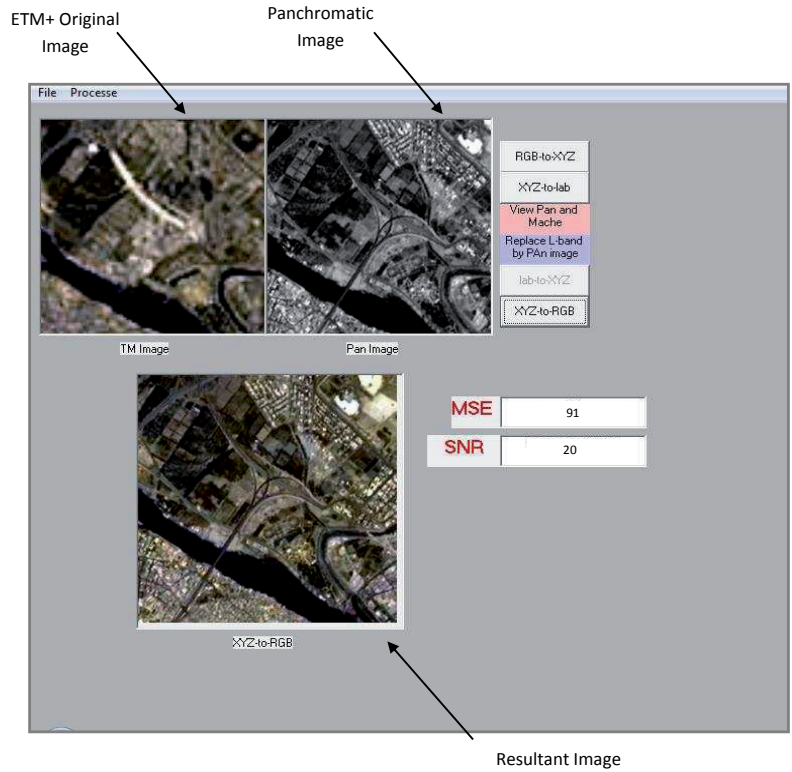

Figure (4.11): Program Interface menu for Lab Fusion method.

YUV space fusion done by

1. Converting Multispectral image from RGB to YUV space

2. Replace Y-band by PAN image

3. Then transform back to yield fused image.

4. Visual basic program Version 6 has been used to test YUV fusion results, fig. (4.12) illustrate the interfacing program.

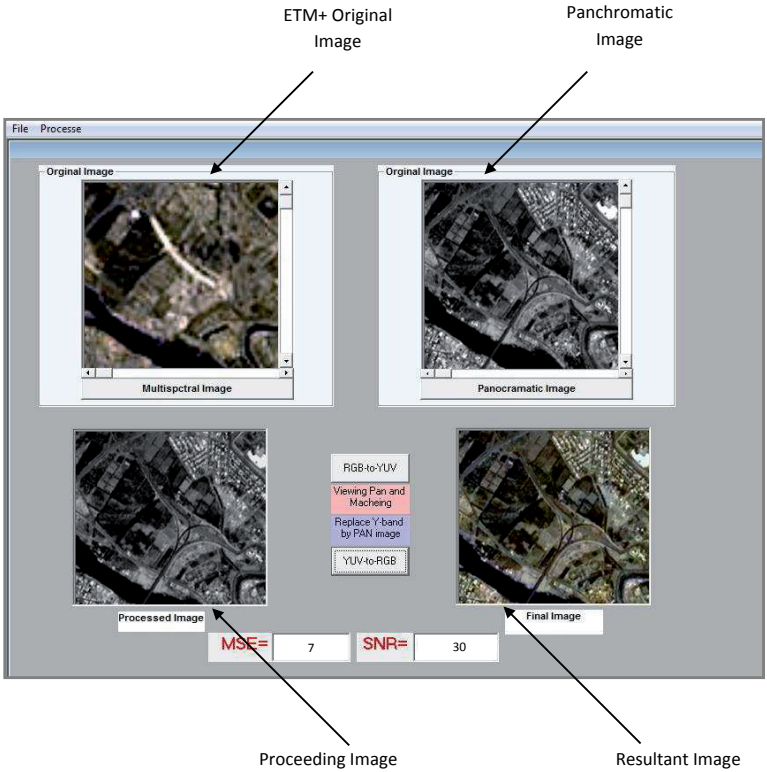

Figure (4.12): Program Interface menu for YUV Fusion method.

(a) ETM+ resized by nearest neighbor method.

(b) HLS method.

(c) ETM+ resized by bilinear method.

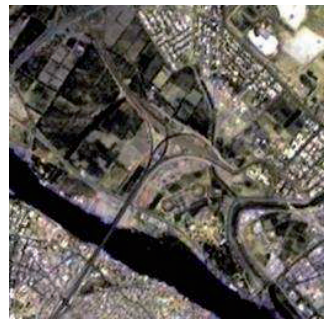

(d) HLS method.

(e) ETM+ resized by Cubic Convolution method.

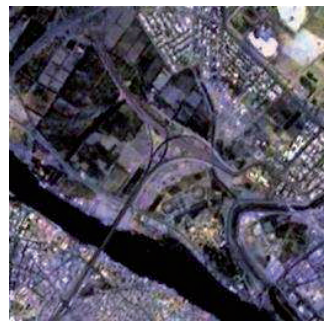

(f) HLS method.

Figure (4.13): left-side represent the resized low-resolution ETM+ images, while the right-side represent the improved fused images, using HLS Transformation method.

(a) ETM+ resized by nearest neighbor method.

(b) Lab method.

(c) ETM+ resized by bilinear method.

(d) Lab method.

(e) ETM+ resized by Cubic Convolution method.

(f) Lab method

Figure (4.14): left half –low resolution MS images, right half fused images by Lab Transformation method.

(a) ETM+ resized by nearest neighbor method.

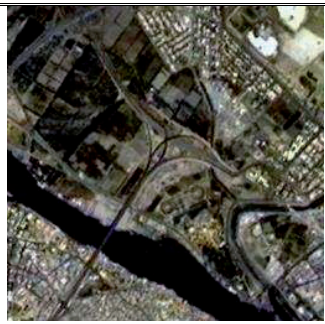

(b) YUV method.

(c) ETM+ resized by bilinear method.

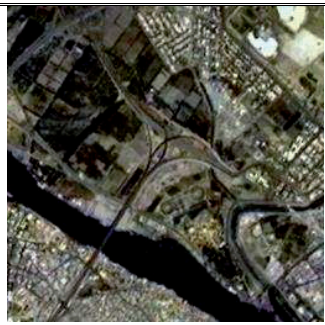

(d) YUV method.

(e) ETM+ resized by Cubic Convolution method.

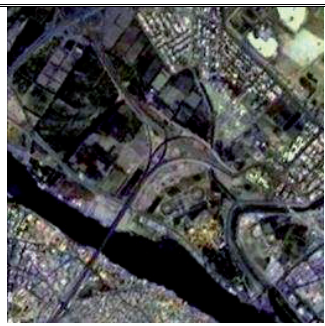

(f) YUV method.

Figure (4.15): left half – low resolution MS images, right half fused images by YUV Transformation method.

4.4 The PCA Fusion Techniques:

PCA transformations have been used to fuse the samples of images, this technique has been implemented in different ways, as illustrated in fig. (4.17); i.e.

1. Implement PCA transforms on multispectral image to product PC1, PC2, PC3..,
2. Replace PC1 by PAN image,
3. Inverse PCA transform to obtain fused image.
4. Visual basic program Version 6 has been used to test PCA fusion results, fig. (4.16) illustrate the interfacing program.

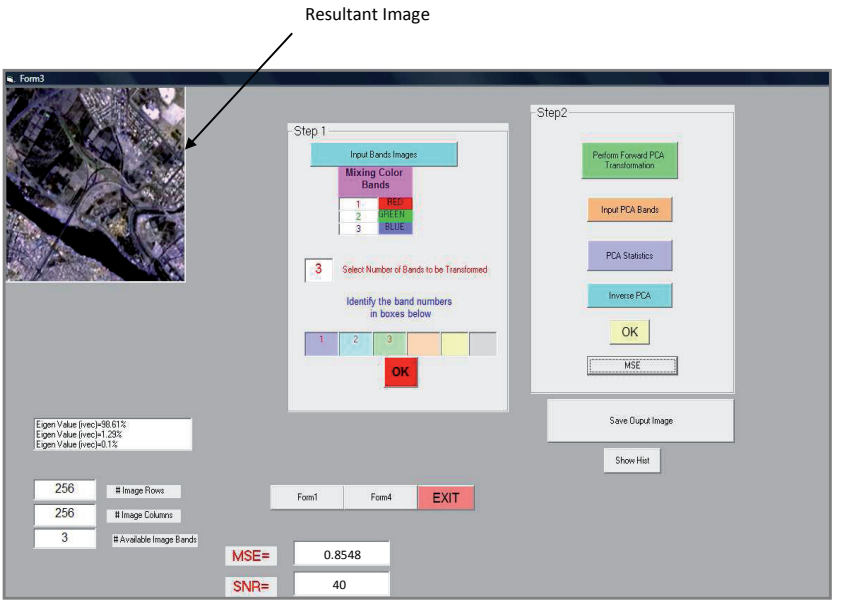

Figure (4.16): Program Interface menu for PCA Fusion method.

(a) ETM+ resized by nearest neighbor method.

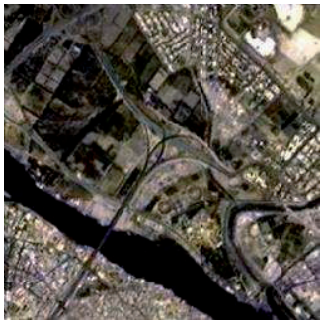

(b) PCA method.

(c) ETM+ resized by bilinear method.

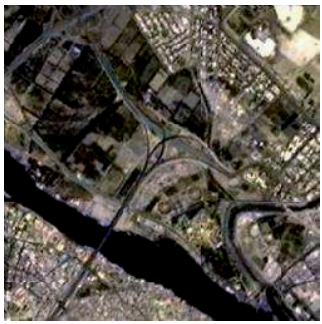

(d) PCA method.

(e) ETM+ resized by Cubic Convolution method.

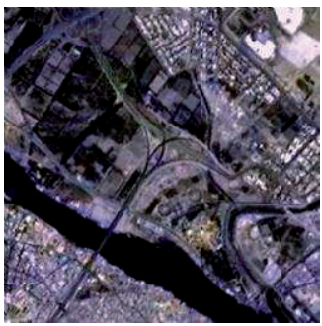

(f) PCA method.

Figure (4.17): left half –low resolution MS images, right half fused images by PCA Transformation method.

The following tables (4-1 → 4-3) represent the quantitative testing measures, in terms of the produced MSE, SNR, and PSNR values.

Table 4-1: Represents the MSE values between the reconstructed fused images with the original PAN.

Type of fusion method	Type of Resembling Methods		
	Nearest Neighbor	Bilinear Interpolation	Cubic Convolution Interpolation
1st level Haar WT	2985	2632	3319
2nd level Haar WT	2376	2177	2803
3rd level Haar WT	1716	2224	1664
1st level TAP 3/5 WT	3163	2777	3459
2nd level TAP 3/5 WT	2618	2373	3001
3rd level TAP 3/5 WT	1959	1887	2803
HLS	5	4	16
Lab	95	91	49
YUV	7	7	474
PCA	1.34	1.35	0.86

Table 4 -2: Represents the SNR measured values between the reconstructed fused images with the PAN.

Type of fusion method	Type of Resembling Methods		
	Nearest Neighbor	Bilinear Interpolation	Cubic Convolution Interpolation
1st level Haar WT	5.2	5.7	4.7
2nd level Haar WT	6.2	6.5	5.4
3rd level Haar WT	6.5	7.7	7.6
1st level TAP 3/5 WT	4.5	5.5	4.9
2nd level TAP 3/5 WT	5.7	6.2	5.2
3rd level TAP 3/5 WT	7	7.2	5.4
HLS	32.8	33	27.7
Lab	20	20.3	23
YUV	30	30	10.3
PCA	38.7	38.6	40.6

Table 4 -3: Represents the PSNR values between the reconstructed fused images with the PAN.

Type of fusion method	Type of Resembling Methods		
	Nearest Neighbor	Bilinear Interpolation	Cubic Convolution Interpolation
1st level Haar WT	13.4	14.2	13.2
2nd level Haar WT	14.4	15	13.2
3rd level Haar WT	15.8	14.9	16.2
1st level TAP 3/5 WT	13	14	13
2nd level TAP 3/5 WT	14.2	14.6	13.6
3rd level TAP 3/5 WT	15.5	15.4	14
HLS	41.4	42.4	36.4
Lab	28.4	28.5	31.2
YUV	39.9	39.9	21.6
PCA	47	47	49

4.5 Conclusions

A variety of fusion techniques have been considered in this thesis; they have been ranged between simplest techniques (based on color transformation) to more complicated method (based on principal component analysis technique). The results, as demonstrated in chapter four have showed differences between the subjective and objective tests, carried on each of them. This may be interpreted because of the reference image was considered as to be the PAN scene, this consideration, definitely, led to incorrect qualification since our fusion goal was to push the degraded scenes (less informatics images) toward the better resolution scenes, and not to make them the same. However, as will be given in the next section (future works), it is helpfully to introducing an alternative test for output image quality. Subjectively, the wavelet-Haar transformation was nastier then the Tap 3/5 because the Low-Low sub-band of the Haar occupies less image energy (i.e. less image information). This was the same for the 2^{nd} and 3^{rd} transformation levels. For the 3^{rd} transformation level, the Tap 3/5 performed better because most of the high frequency information's were preserved at the High-Low, Low-High, and the High-High sub images.

Generally, the color transform fusion techniques improved better than the wavelet techniques, this could be interpreted by the amount of energy preserved at the replaced color band than that at the wavelet sub-band. However, the YUV color transformation showed better quality than other color transformation, which means that this transformation produced less correlated information than other transformations; i.e. as the transform produce less correlate information means yield higher compacted image energy in few component.

It was very obvious, that the PCA technique yields a very sophisticated result than the previously mentioned (color and wavelet transformations). This transformation, as can be seen at the most literature is considered as an optimum because of its de-correlation and its energy compaction.

4.6 Suggestions for future works:

- There are many other wavelet transformation method have been developed for different applications (among these are Dubshies, the Tap 7/9, etc). Implementing one of these may led to an improve fusion result.
- We can use a wavelet transform to fuse a Landsat ETM+ image with SPOT panchromatic image with proposed a replacement fusion rule for the high

frequencies parts of the wavelet transforms of the images, with keeping the low frequency part intact.

- HSI-based image fusion introduces serious color distortions in the final product, i.e. the color of the object may change during the fusion. It has been shown that the changes in color mainly arise from the changes in saturation during the fusion process. The S- (Saturation) band may be treated different to keep the final result color unchanged. This is partially manipulated in our research; an additional normalization method may improve the final result.

References

References

[App 1996]
Apple Computer, "*Advanced Color Imaging on The Mac OS*", 1999.
http://developer.apple.com/membership/
[Are 2003]
Paul Arellano, *"Missing information in the remote sensing: Wavelet approach to detect and remove clouds and their shadows"*, International Institute of Information Science and Earth Observation, Enschede, March 2003.
http://www.itc.nl/library/papers_2004/msc/gfm/arellano
[Aub 2007]
Nawal Khalf Ghazal Al-Aubaidi, *"Producing 3D-Photomaps from Mosaic Aerial Digital Stereo-Image"* Dr Thesis in Physics, Baghdad University, college of Science, physics department 2007.
[Azz 2001]
Eman Fathel Al-Azzawi, *"Satellite Image Processing For (GIS) Application"*, Dr. Thesis in Physics, Baghdad University, college of Science, physics department, 2001.
[Bou 1994]
Bourke P, *"Ccfolor Space FAQ"*, graphics/colorspace-faq, 1994.
http://www.ncveuro.sfc.keio.ac.jp/~aly/polygon/info/color-space-faq.htm
[Bre 2000]
Bretschneider T,Kao O, *"Image Fusion in Remote Sensing "*, Proceeding of the 1st online, symposium of Electronic Engineers, 2000.
[Bun 2004]
Vladimir Buntilov, *"Image and Information Fusion in Remote Sensing"* First Year Progress Report, school of computer Engineering, 2004.
[Cam 1996]
James B.Campbell, *"Introduction to Remote Sensing"*, 2nd Edition, Taylar& Francis Ltd 1996.
[Cha 1991]
Chavez, P. S., Sides, S. C., and Anderson, J. A., *"Comparison of three different methods to merge multiresolution and multispectral data: TM & SPOT pan"*. Photogrammetric Engineering and Remote Sensing, Vol. 57, pp. 295-303, 1991.
[Cra 1999]
Crawford, M, M, Kumar, S.,Richard ,M.R.,Giberaut ,Je and Schwander,A.N. *"Fusion of Airborne Palarimetric and Interferometric SAR for Classification of Coastal Environments"* IEEE Tran.Geosci&Engg .vol.39, No 3, pp.1306-1315, 1991.
[ERD 8.7]
ERDAS Field Guide,7th Edition, Leica Geosystems GIS & Mapping, LLC, 2003.

[Fau 1989]
Faust, N. L. *"Image Enhancement"*, Vol.20, Supplement 5 of Encyclopedia of Computer Science and Technology. Ed.A. Kent and J. G. Williams. New York: Marcel Dekker, Inc., 1989.
[For 1998]
Adrian Ford and Alan Roberts *"Color Space Conversion"*, August 11, 1998.
(Ajoec1@wmin.ac.uk<defuncf>)(Alan.Roberts@rd.bb.co.ul).
[Gar 1996]
Garguct. Duport, B.,J.Girel,J.M.Chassery and G.Pautou *"The Use of Multi-resolution Analysis and Wavelet Transform for Merging Spot panchromatic and multispectral image Data"* Photogrammetric Engineering and Remote Sensing.,Vol.62 No.9, pp. 1057–1066, 1996.

[Gon 1977]
R.C.Gonzales and P.Wintz, Addison Wesley, *"Digital Image Processing"*, 1st edition, publishing company, 1977.
[Gon 1987]
R. C. Gonzales, and P. Wintz, *"Digital Image Processing"*, 2nd. Edition, Addision-Wesly Publishing Company, 1987.
[Gon 2002]
Gonzalez R.C. and Woods R.E. *"Digital Image Processing"* 2nd Edition, Prentice-Hall, Inc,2002.
[Gra 2004]
Grant, A.; Meadows, J. *"Satellites Communication"*, Communication Technology Update, 9th Edition, Burlington: Focal Press, 2004.
[Gro 1998]
Gross, H.N, and Schoote, J.R., *"Application of Spectral Mixture Analysis and Image Fusion Techniques for Image Sharpening"*, Remote Sensing of Environment, vol.63, pp 85-94, 1998.
[Had 2001]
Firas Abdul-Razzaq Hadi, *"Image Deblurring Using Orthogonal Polynomials"* Msc Thesis in Astronomy, Baghdad University, college of science, Astronomy department, 2001.
[Ind 2005]
Map India, *"Image Fusion in GRDSS for Land Use Mapping"*, Map India 2005, Geomedia 2005.www.mapindia.org/2005/papers/66.pdf
[Jab 2006]

Hameed Majeed Abul Jabar, *"Fusion Techniques for Globalizing the Features of satelitte Images"*, Dr Thesis in Physics, Baghdad University, college of Education (Ibn AL-Haitham), physics department 2006.

[Jen 1996]

Jensen, J.R., *"Introductory Digital Image processing"*, a remote sensing perspective, 2nd Edition, Prentice Hall., 1996.

[Kaf 2003]

Valerie Kaftandjian, *"Use of Data Fusion Methods to Improve Reliability of Inspection: Synthesis of the work done in the frame of a European Thematic Network."*.NDT net-February 2003, vol.8, No.2, (INSA-CNDRI, France), 2003.

[Kan 2001]

H.H.Kang,J.H.Park, *"Image Fusion Watermarking Based on the Discrete Wavelet Transform"* Proc. of Int'l symposium on Advanced Engineering pp.377-386, 2001.

[Lew 1990]

Rhys Lewis, *"Practical Digital Image Processing"* by Ellis Horuood Limited Published, 3rd Edition, Great Britain, 1990.

[Li 2000]

Li .L, and sheng, Y. *"Improving Spatial Resolution of IR Image by Means of Sensor Fusion"*, URL, 2000. http://www.tropin.phy.uiaval.ca/jli.

[Li 2002]

Li S, Kwok J. T, Wang Y, *"Using the Discrete Wavelet Frame Transform to Merge Landsat TM and SPOT Panchromatic Images"*, Information Fusion, Vol. 3, Issue 1, pp. 17-23, March 2002.

[Lia 1999]

Liao Y, Wang T, Zheng W, *"Quality Analysis of Synthesized High Resolution Multispectral Imagery"*, Department of Surveying Engineering, National cheng Kung university, University Road1, Tainan, Taiwan, 1999.
http://www.gisdevelopment.net/aars/1998ts9/ts9001.shtml

[Lie 2001]

Liew S. C, *"Principles of Remote Sensing",* Centre for Remote Imaging, Sensing and Processing, National University of Singapore, 2001. www.crisp.nus.edu.sg.

[Log 2005]

Logcal S.r.l, the Easy RGB site, copyrights 2005.http://www.easyrgb.com/index.htm/

[Mal 1987]

Mallat, S., "*A Compact Multiresolution Representation: The Wavelet Model"* Proc. IEEE Computer Society Workshop on Computer Vision, IEEE Computer Society Press, Washington, D. C, pp. 2-7, 1987.

[Mat 6.5]
The Math Works Inc. "*MATHLAB - The Language of Technical Computation"*, Version 6.5, Release Date: 18 June 2002.
[Moh 1997]
Mohanty K.K and Madjumdar, T.J., *"A Comparison of IRS-1C.Panchromatic and LISS III data Fusion Using Adaptive Filtering, HIS and Fourier Transform."*, In ISRS and NNRMS Bulletin. (Rem.Sen.for Nat.Res.), pp. 420-429, 1997.
[Moh 2006]
Faisel Ghazee Mohammed, *"Color Image Compression Based on DWT"*, Dr. Thesis in Astronomy, Baghdad University, college of science, Astronomy department, 2006.
[Moo]
Aaron Moody, *"Remote Sensing of The Environment: Remote Sensing Resolutions"* Department of Geography, University of North Carolina.
http://www.unc.edu/~aaronm/RSCC/FIG1.html
[Nib 1986]
Wayan Niblack*,"An Introduction to Digital Image Processing"*, Prentice-Hall International (UK) Ltd, 1986.
[Nic 2007]
Nicolas M.Short, Sr.*,"Introduction: Technical and Historical Perspectives of Remote Sensing"* June, 18, 2007.
[NRC 2007]
Natural Resources Canada, *"Fundamentals of Remote Sensing"*, A Canada Center for Remote Sensing, Remote Sensing Tutorial, 2007.
www.nrcan.gc.ca
[Paj 2004]
Pajares, G.,and Cruz,J.M.d.L*,"A wavelet-Based Image Fusion Tutorial"*, The Journal of the Pattern Recognition Society, vol.37, pp1855-1872, 2004.
[Pol 1998]
Pohl C, and Van Genderen J, *"Review Article: Multisensor Image Fusion in Remote Sensing: Concepts .Methods and Applications"* Int.j.remote sensing, vol.19, no.5, pp 823-854, 1998.
[Rec 1998]
John A. Rechards, *"Remote Sensing Digital Image Analysis: An Introduction"*, 3rd Edition, Xiuping Jia, 1998.
[Roc 1998]
Rockinger O, Fechner T, *"Pixel-Level Fusion: The Case of Image Sequences"*, SPIE Proceedings, 1998, vol.3374, pp.378-388.
[RSN 1993]
Remote Sensing Note, Japan Association on Remote Sensing, 19.5.1993.

http://shiba.ii.u-toko.ac.jp/jars/JARS1.html
[Sab 1978]
Floyd F. Sabins, *"Remote Sensing a Principle and Interpretation"*, chevron oil field research company, university of southern California and university of California, Los Angeles 1st Edition, 1978.
[Sal 2004]
David Salmon, *"Data Compression"* 3rd Edition, Springer Verlag New York, Inc, 2004.
[San 2001]
S. Sanjeevi, K. Vani and K. Lakshmi, *"Comparison of Conventional and Wavelet Transform Techniques for Fusion of IRS-ICLISS and PAN Image"*, 22nd Asian Conference on Remote Sensing, 5-9 November 2001 Singapore.
[She]
Shefali Aggarwal, *"Principles of Remote Sensing"*, Photogrammetry and Remote Sensing Division,Indian Institute of Remote Sensing, Dehra Dun.
http://www.wamis.org/agm/Pubs/agm8/paper-2.pdf
[Shm 1999]
Wafaa K.Shmes, *"Adaptive principle Components Methods for Image Classification and Compression"* MSC. Thesis, University of Baghdad, College of Science, 1999.
[Sta 1998]
Stark J., Murtaghf, and Bijaoui A, *"Image Processing and Data Analysis: The Multiscale Approach"* Cambridge University Press, 1998.
[Umb 1998]
Scott E Umbaugh, *"Computer Vision and Image Processing"*, A partial Approach Using CVIP tools, Ph.D.1998.
[Ven 2002]
Ventura, F. N., Fonseca, L. M. G., Santa Rosa, A. N. C. *"Remotely sensed image fusion using the Wavelet Transform: International Symposium on Remote Sensing of Environment"*, Buenos Aires, 29, 2002.*Proceedings.* 4p.
[Wik 2005]
"Color Space", Wikipedia Free Encyclopedia, 2005.
http://en.wikipedia.org/wiki/mainpage.
[Wik 2008]
"SPOT Satellites", Wikipedia, The Free Encyclopedia ,2008.
http://en.wikipedia.org/wiki/Spectral_resolution
[Wik]
USSR, Wikipedia,*http://en.wikipedia.org/wiki/Image:Sputnik_asm.jpg*.

الملخص

تعرف عملية دمج البيانات على أنها آلية لتوحيد ووضع معلومات سبق وان تم الحصول عليها من متحسسات مختلفة والعائدة لمجموعة من محطات الرصد في صورة مركبة واحدة. إن البحوث التي تناولت موضوع توحيد البيانات تركز اهتمامها من اجل تطوير نماذج جديدة وملائمة لدمج مدى مختلف ومعقد من البيانات الصورية.

في هذا البحث، استخدمت العديد التقنيات لغرض تحسين وتطوير المعلومات في الصور ذات الدقة الواطئة والتي تم تحسسها عن بعد، بالاستفادة من الصور ذات الدقة العالية والأحدث ولنفس الموقع.

إن طرق التوحيد المستخدمة هي:

1- تقنيات التوحيد القائمة على عمليات التحويل المويجي؛ حيث تم توظيف كل من تقنية Haar و Tab3/5 ولعدة مستويات من التحويل. ويمكن ذلك من خلال استبدال المركبة Low-Low للصورة الواطئة الدقة بنظيرتها من المستوى المقابل لمركبة التحويل Low-Low للصورة عالية الدقة. بعدها يتم تطبيق طريقة عكس التحويل لاستعادة الصور المحسنة.
2- تم استخدام ثلاث طرق تحويل لوني لمعالجة حالة ضعف الدقة للصور المتحسسة عن بعد؛ حيث تم استخدام أساليب التحويل اللوني YUV, HLS, Lab لغرض التوحيد. ان الحزمة اللونية الأكثر فعالية (L- band) والعائدة لكل من تحولات HLS, Lab وكذلكY في YUV، قد تم استبدالها بمشاهد الدقة العالية والمتمثلة بحزمة Panchromatic لصورة القمر SPOT. بعدها يتم تطبيق طريقة عكس التحويل لاستعادة الصور المحسنة.
3- استخدمت أيضا تقنية PCA للقيام بعملية التوحيد أو الدمج. وتعد طريقة التحويل هذه هي الطريقة المثلى، أي بمعنى إنها تؤدي إلى تحقيق أعلى درجة من عدم الترابط. حيث يستبدل المستوى الأول من هذا التحويل للصورة ذات الدقة الواطئة بالصورة ذات الدقة العالية Panchromaticوالمأخوذة من القمر SPOT. ومن ثم تطبق طريقة PCA العكسية لغرض استرجاع الصورة المحسنة.

تم اختبار جودة الصور الموحدة عيانيا، من خلال عرض النتائج المستحصل عليها؛ وكميا من خلال قياس متوسط مربع الخطأ (MSE)، ونسبة الإشارة إلى التشويش (SNR)، بالإضافة إلى أعلى درجة للإشارة إلى التشويش (PSNR) للصور الناتجة وبالمقارنة مع مثيلتها من الصور ذات الدقة العالية Panchromatic والمأخوذة من القمر SPOT.